Nucleon and $\Delta(1232)$ form factors at low momentum transfer and small pion masses

T. Ledwig,[1,*] J. Martin-Camalich,[2] V. Pascalutsa,[1] and M. Vanderhaeghen[1]

[1]*Institut für Kernphysik, Johannes Gutenberg-Universität, D-55099 Mainz, Germany*

[2]*Departamento de Fisica Teorica and IFIC, Universidad de Valencia-CSIC, Spain and Department of Physics and Astronomy, University of Sussex, BN1 9Qh, Brighton, UK.*

(Received 1 September 2011; published 8 February 2012)

An expansion of the electromagnetic form factors of the nucleon and $\Delta(1232)$ in small momentum transfer and pion mass is performed in a manifestly covariant EFT framework consistent with chiral symmetry and analyticity. We present the expressions for the nucleon and $\Delta(1232)$ electromagnetic form factors, charge radii, and electromagnetic moments in the framework of $SU(2)$ baryon chiral perturbation theory, with nucleon and Δ-isobar degrees of freedom, to next-to-leading order. Motivated by the results for the proton electric radius obtained from the muonic-hydrogen atom and electron-scattering process, we extract values for the second derivative of the electric form factor which is a genuine prediction of the p^3 BχPT. The chiral behavior of radii and moments is studied and compared to that obtained in the heavy-baryon framework and lattice QCD. The chiral behavior of $\Delta(1232)$-isobar properties exhibits cusps and singularities at the threshold of $\Delta \to \pi N$ decay, and their physical significance is discussed.

DOI: 10.1103/PhysRevD.85.034013 PACS numbers: 12.39.Fe, 13.40.Em, 25.20.Dc

I. INTRODUCTION

The physics of nucleon form factors is about 60 years old [1,2] and yet surprises in this venue are not unusual till now. Just last year the most precise atomic measurement of the proton charge radius yielded [3]: $r_{Ep} = \sqrt{\langle r^2 \rangle} = 0.84184(67)$ fm, in unexpected disagreement with the best electron-scattering result [4]: $r_{Ep} = 0.879(8)$ fm. Much effort since then have been focused on finding a ''missing'' correction in the muonic-hydrogen result, e.g. [5–8]. We, on the other hand, will attempt to provide here some grounds for an improvement of the electron-scattering analysis. The electron-scattering measurement of the proton charge radius is done by determining the slope of the proton form factors at zero momentum transfer: $Q^2 \equiv -q^2 = 0$. In reality the measurements are done at small but finite momentum transfer, $Q^2 \geq 0.01$ GeV^2, and an interpolation to zero is required. The simplest one is based on Taylor expansion in Q^2,

$$G_{Ep}(Q^2) = 1 - \frac{\langle r^2 \rangle}{6} Q^2 + \frac{\langle r^4 \rangle}{120} Q^4 + \ldots, \qquad (1)$$

where $\langle r^n \rangle$ is the nth moments of the proton charge distribution which values are fitted to data. However, the validity of such an expansion, its radius of convergence, is limited by the nearest singularity in the complex Q^2 plane, which, if we neglect the radiative corrections, is located at $Q^2 = -4m_\pi^2$, the two-pion production threshold. This simply means that a polynomial fit is limited to $|Q^2| \ll 4m_\pi^2 \approx 0.08$ GeV^2, where the database is scarce. One can extend the interpolation range only by including the effect of the pion-production channels explicitly. This can in principle be done using dispersion theory, see e.g. [9–11]. For that, however, one needs the information in the timelike region, which is also not accurate enough, and is usually complemented in a model-dependent fashion. Nonetheless, some of the state-of-the-art dispersion analyses [12,13] had obtained the smaller value of r_{Ep} (well before the muonic hydrogen result appeared!), which reinforces the motivation to include the pion-production effects in the interpolation of low-Q^2 data. Here we approach this issue in the framework of chiral perturbation theory (χPT) [14,15]. The χPT itself does not have a prediction for the proton charge radius, its leading-order value is given by a combination of low-energy constants (LECs), which are free parameters of the theory to be matched to QCD. However, the leading order pion-loop contributions are fixed in terms of well-known parameters and provide a prediction of the analytic structure of the form factors at small Q^2. In this work we shall only present the relevant χPT calculations; their impact on the charge radius extraction will be studied elsewhere.

Another set of issues concerning the electromagnetic form factors comes from the side of lattice QCD, which presently is the only method to do *ab initio* calculations of the low-Q^2 hadron structure. The latest lattice QCD calculations of the nucleon [16–20] and $\Delta(1232)$ [21–25] electromagnetic (e.m.) properties call for a better analysis of the pion-mass and volume dependencies. The most troublesome are the results for the nucleon charge radii, which show little dependence on the pion mass and a large discrepancy with experiment upon a naive extrapolation to the physical pion mass. χPT predicts charge radii to diverge in chiral limit ($m_\pi \to 0$) and therefore from its point of view it is plausible that the correct chiral extrapolation and finite-volume corrections will reconcile the lattice results with experiment.

*ledwig@kph.uni-mainz.de

Presently, both m_π and finite-volume dependencies are usually computed using the heavy-baryon χPT (HBχPT) [26], where the chiral expansion is accompanied with an expansion in the inverse baryon mass. The latter expansion can be poorly convergent (see, e.g. [27,28]) and the so-called manifestly Lorentz-invariant schemes [27,29], which avoid the heavy-baryon expansion, gain popularity in practice. In this work we adopt the extended on-mass shell scheme (EOMS) [30], which has the advantage of preserving analyticity. As a result, our expressions for the form factors will satisfy the usual dispersion relations written in Q^2, as well as the dispersion relation of Ref. [31] written in m_π^2:

$$G(Q^2, m_\pi^2) = \frac{1}{\pi}\int_0^\infty dq^2 \frac{\mathrm{Im}\, G(-q^2, m_\pi^2)}{q^2 + Q^2}\left(\frac{-Q^2}{q^2}\right)^n \tag{2a}$$

$$= -\frac{1}{\pi}\int_{-\infty}^0 d\tilde{m}_\pi^2 \frac{\mathrm{Im}\, G(Q^2, \tilde{m}_\pi^2)}{\tilde{m}_\pi^2 - m_\pi^2}\left(\frac{m_\pi^2}{\tilde{m}_\pi^2}\right)^n, \tag{2b}$$

where 0 in the integration limits is indicative of the threshold position, n is the number of subtractions; Q^2 and m_π^2 are positive. The earlier χPT analyses of nucleon and Δ-isobar form factors were based on either the heavy-baryon approach [32,33], or the infrared-regularization scheme [34], where the above dispersion relations can only be satisfied approximately, unless a special care is taken as, e.g., in [35]. Reference [36] contains thus far the only $SU(2)$ calculation of nucleon form factors in the EOMS whereas calculations of the octet- and decuplet-baryon em moments has been reported in the context of $SU(3)$ BχPT in [37–39]. Here we have recalculated the contributions found in [36], included the leading-order corrections due to Δ-isobar, and computed all the $\Delta(1232)$-isobar form factors to next-to-leading order.

In Sec. II, we summarize the ideas of chiral expansion in the single-baryon sector and specify the contributions calculated in this work. In Sec. III and IV we consider the pion-mass dependence of, respectively, the nucleon and Δ electromagnetic radii and moments, and compare it with the HBχPT results and lattice-QCD results where possible. In Sec. V we investigate some higher order effects to our results and summarize this work in Sec. VI. Appendix A contains the notation and definitions, while Appendices B and C contain analytical expressions of the contributions to, respectively, the nucleon and the Δ form factors obtained in this work.

II. FORM FACTORS IN BARYON χPT

The chiral effective-field theory to which we refer as to χPT is an effective-field theory of low-energy QCD, as it contains the most general form of interaction among the lightest hadrons—most notably, pions—in a way consistent with symmetries of QCD Green's functions [14,15]. A special role is enjoyed by chiral symmetry which insures that pions couple through a derivative couplings while the symmetry breaking terms are accompanied with powers of m_π^2. When the scale of spontaneous chiral symmetry breaking, $4\pi f_\pi \approx 1$ GeV, is much larger than the scale of the explicit symmetry breaking, m_π, as is observed in nature, one may set up a systematic expansion of any observable quantity in powers of $E/(4\pi f_\pi)$ and $m_\pi/(4\pi f_\pi)$, where E is the characteristic relative-energy of external legs in a given process. These ratios of light to heavy scales are commonly denoted as p. To a given order in p, a finite number of terms, accompanied by a finite number of low-energy constants (LECs), contribute. Simple power-counting rules exist to select the necessary contributions to any given order in p.

A. Power counting in the single-baryon sector

The inclusion of the nucleon fields was initially done by Gasser, Sainio and Svarc [40], who note that the nucleon mass M_N invalidates the usual power-counting arguments. For instance, the one-loop nucleon self-energy graph, with the leading πNN couplings, counts as order p^3, but in the actual calculation the positive powers of M_N appear and make this contribution of order p^2. It was later on realized that such ''power-counting violating'' terms have no physical effect since their contribution is always compensated by LECs present at that order in the expansion of physical quantity [29]. One can set up a scheme where the troublesome terms are absorbed by a renormalization of available LECs, e.g. the EOMS [30].

A neat way to get rid of positive powers of M_N from the outset is provided by the HBχPT [26]. In HB expansion, which is in a way similar to semirelativistic treatments, in addition to the positive power of M_N one drops a number of contributions with negative power of M_N. These contributions are typically of the form

$$\left(\frac{m_\pi}{M_N}\right)^n \left[a + b\ln\frac{m_\pi}{M_N}\right], \tag{3}$$

with n higher than the order of p to which the expansion is made. As long as the constants a and b are of order of unity (natural size) relative to the coefficients of the given-order term, these terms are indeed of the size of higher-order corrections. There are examples, however, where a, b are unnaturally large and the expansion fails as the result (see, e.g. [27,28]). In these cases, the expansion in p might only converge if one refrains from the HB expansion.

A popular manifest-Lorentz-invariant scheme where the power-counting-violating terms do not arise is the infrared regularization (IR) of Becher and Leutwyler [27], which has been applied to nucleon form factors by Kubis and Meissner [34]. The IR procedure can be described as follows.

(i) *An equivalent formulation of the IR:* The negative-pole contribution of nucleon propagator in a give loop graph is deleted by hand. As the result, the graphs with nucleon propagators only vanish, since

the contour can always be closed in the half-plane which does not have a pole. In the graphs where both the nucleon propagators enter with a pion propagator, e.g.,

$$S_\pi(k)S_N(p) \equiv \frac{1}{k^2 - m_\pi^2}\frac{\not{p} + M_N}{p^2 - M_N^2} \tag{4}$$

the nucleon propagator is replaced as follows:

$$S_N(p) \to \frac{\not{p} + M_N}{p^2 - M_N^2 - S_\pi^{-1}(k)} = S_N(p)\left[1 + \frac{1}{S_\pi(k)(p^2 - M_N^2)}\right]. \tag{5}$$

In any one-loop graph containing N_π pion propagators,

$$S_\pi(k_1)\cdots S_\pi(k_{N_\pi}), \tag{6}$$

each nucleon propagator changes as follows:

$$S_N(p) \to S_N(p)\left[1 - (-1)^{N_\pi}\prod_{n=1}^{N_\pi}\frac{1}{S_\pi(k_n)(p^2 - M_N^2)}\right]. \tag{7}$$

This formulation is more convenient to check Ward-Takahashi identities since the normal propagator preserve gauge invariance and the additional part vanishes upon closing the loop integration contour in the half-plane which is free of poles. It is not difficult to see that the ''modified'' IR procedure [41], introduced to define IR beyond one loop, does not satisfy the e.m. gauge symmetry exactly, but only to a given order in the chiral expansion. The violating terms are of higher order from the viewpoint of heavy-baryon expansion, but not in a covariant framework.

One apparent drawback of IR is that it changes the analytic structure of the loop integrals such that unphysical cuts appear. The unphysical cuts lie far outside the region of χPT interest, but they still have an effect on that region as can be seen, for example, through a dispersive representation. Namely, if the quantity in question obeys a dispersion relation, let say in energy s,

$$G(s) = \frac{1}{\pi}\int_{s_0}^{\infty} ds' \frac{\mathrm{Im}\, G(s')}{s' - s}, \tag{8}$$

then in the IR scheme it would take the form:

$$G^{(\mathrm{IR})}(s) = \frac{1}{\pi}\int_{s_0}^{\infty} ds' \frac{\mathrm{Im}\, G(s')}{s' - s} + \frac{1}{\pi}\int_{-\infty}^{f_0} ds' \frac{\mathrm{Im}\, G^{(\mathrm{IR})}(s')}{s' - s}, \tag{9}$$

such that, even if f_0 is far away from the region of interest (i.e., $f_0 \ll s$ and $s \approx s_0$), an unphysical contribution is generated and its smallness is hard to assess *a priory*. The imaginary part over the physical cut is the same in IR, EOMS, or any other relativistic scheme. In fact, the whole difference between the IR and EOMS is the unphysical cut contribution.

A common problem of Lorentz-covariant schemes is that the superficial index of divergence ω may exceed the chiral power-counting index n, and thus an UV-divergence may appear $\omega - n$ orders lower than the LEC which renormalizes it. This problem is often viewed as an inconsistency of the covariant approach, but in fact it only means one needs to specify the renormalization scheme for all LECs from the outset. In HBχPT, $\omega = n$, because the time-derivatives of the heavy (nucleon) field are eliminated. On the other hand, the HBχPT results can readily be reproduced from covariant ones by expanding the latter in the inverse baryon masses.

Since the nucleon is easily excited into the $\Delta(1232)$-resonance, the excitation energy $\Delta = M_\Delta - M_N \ll 4\pi f_\pi$, the χPT with nucleons is not complete without the Δ-isobar degrees of freedom. The power-counting for the Δ-isobar contributions depends on how the two light scales m_π and Δ compare to each other. $m_\pi \sim \Delta$ leads to the ''small-scale-expansion'' (SSE) [42], while $m_\pi \ll \Delta$ leads to the ''δ-expansion'' [43,44]. In the absence of one-particle-reducible graphs, as is in the case of form factors, the two power-countings yield very similar results. In the δ-expansion, where a one-particle-irreducible graph with L loops, N_π pion propagators, N_N nucleon propagators, N_Δ

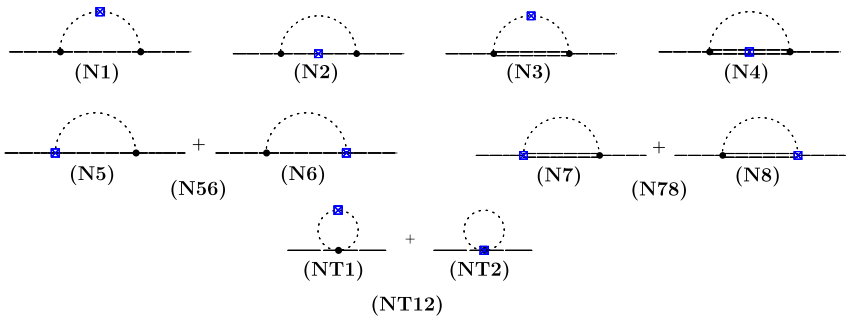

FIG. 1 (color online). Order-p^3 corrections to the nucleon form factors. Single-lines denote the nucleon, double-lines the Δ-isobar, and dashed lines the pion propagators. The photon coupling is denoted by the blue square and the $N\pi$ or $\Delta\pi$ vertices by dots.

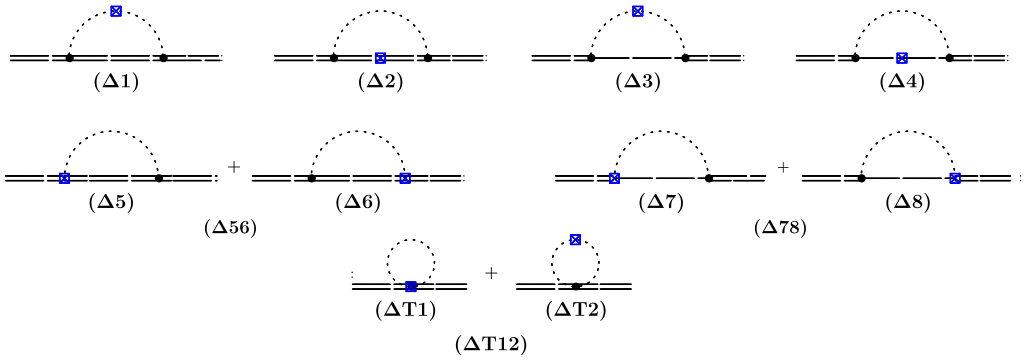

FIG. 2 (color online). Order-p^3 corrections to the Δ-isobar form factors.

propagators, and V_k vertices containing k powers of pion momentum (and electric charge), counts as:

$$p^{4L-2N_\pi-N_N-N_\Delta-\sum_k kV_k}\left(\frac{p}{\Delta}\right)^{N_\Delta}. \tag{10}$$

In the SSE the power-counting index of such graphs would be

$$p^{4L-2N_\pi-N_N-N_\Delta-\sum_k kV_k}, \tag{11}$$

and hence for $p\sim\Delta$ the two countings coincide. The pion mass insertions which are relevant for the pion-mass-dependence calculation will still render the countings to be different. In this case, however, the δ-expansion is not appropriate as the pion-mass dependence needs usually to be assessed in the range of $m_\pi\sim\Delta$. For this purpose we adopt the SSE counting.

In this work we have calculated the p^3 graphs shown in Figs. 1 and 2. The resulting expressions are collected in Appendix B and C, respectively. Below we list the terms of the effective chiral Lagrangian that were used in the calculation of these loops.

B. Details of the effective Lagrangian and loop results

The effective Lagrangian is written in terms of pion, nucleon, Δ-isobar and photon fields, π^a, N, Δ_μ, A_μ, and—expanded to the appropriate power in the number of these fields, pion derivatives and mass—reads as follows:

$$\begin{aligned}
\mathcal{L} &= \mathcal{L}_N^{(1)}+\mathcal{L}_\Delta^{(1)}+\mathcal{L}_{\Delta N\pi}^{(1)}+\mathcal{L}_\pi^{(2)},\\
\mathcal{L}_{N\pi}^{(1)} &= \bar N(\not D - M_N)N-\frac{g_A}{2f_\pi}\bar N\tau^a(\not D^{ab}\pi^b)\gamma_5 N,\\
\mathcal{L}_{\Delta\pi}^{(1)} &= \bar\Delta_\mu(i\gamma^{\mu\nu\alpha}D_\alpha - M_\Delta\gamma^{\mu\nu})\Delta_\nu\\
&\quad+\frac{H_A}{2f_\pi M_\Delta}\varepsilon^{\mu\nu\alpha\lambda}\bar\Delta_\mu\mathcal{T}^a(D_\alpha\Delta_\nu)D_\lambda^{ab}\pi^b\\
\mathcal{L}_{\pi\Delta N}^{(1)} &= i\frac{h_A}{2f_\pi M_\Delta}\bar N T^a\gamma^{\mu\nu\lambda}(D_\mu\Delta_\nu)(D_\lambda^{ab}\pi^b)+\text{h.c.},\\
\mathcal{L}_\pi^{(2)} &= \frac{1}{2}(D_\mu^{ab}\pi^b)(D_{ac}^\mu\pi^c)-\frac{1}{2}m_\pi^2\pi_a\pi^a,
\end{aligned} \tag{12}$$

where the definitions of the isospin and Dirac matrices are given in Appendix A and the covariant derivatives are:

$$\begin{aligned}
D_\mu^{ab}\pi^b &= \delta^{ab}\partial_\mu\pi^b+ieQ_\pi^{ab}A_\mu\pi^b,\\
D_\mu N &= \partial_\mu N+ieQ_N A_\mu N+\frac{i}{4f_\pi^2}\epsilon^{abc}\tau^a\pi^b(\partial_\mu\pi^c),\\
D_\mu\Delta_\nu &= \partial_\mu\Delta_\nu+ieQ_\Delta A_\mu\Delta_\nu+\frac{i}{2f_\pi^2}\epsilon^{abc}\mathcal{T}^a\pi^b(\partial_\mu\pi^c),
\end{aligned} \tag{13}$$

with $e>0$. Further details can be found in Sec. 4 of Ref. [45].

The parameters of the Lagrangian are considered to be known and their physical values are listed in Table I. The value of $H_A=(9/5)g_A\simeq 2.28$ is taken from the large-N_c limit and the value of $h_A=2.85$ is fixed by the experimental $\Delta(1232)$-isobar decay width $\Gamma_\Delta=0.115$ GeV, cf. [46].

The couplings to the Δ-isobar are chosen to be consistent with the covariant construct of the free Rarita-Schwinger theory and hence do not invoke the unphysical degrees of freedom of vector-spinor field [47–49]. However, the minimal coupling of the photon, here the $\gamma\Delta\Delta$ coupling, is the well-known exception. We attempt to correct this problem by adding nonminimal $\gamma\Delta\Delta$ coupling [23,50]:

$$\mathcal{L}_{\gamma\Delta\Delta}^{\text{nm}}=\frac{e}{M_\Delta}\bar\Delta_\mu(i\kappa_1F^{\mu\nu}-\kappa_2\gamma_5\tilde F^{\mu\nu})\Delta_\nu, \tag{14}$$

where $F^{\mu\nu}=\partial^\mu A^\nu-\partial^\nu A^\mu$ and $\tilde F^{\mu\nu}=\varepsilon^{\mu\nu\rho\lambda}\partial_\rho A_\lambda$ are the electromagnetic field strength tensor and its dual with $\varepsilon_{0123}=+1$. This nonminimal coupling, for $\kappa_1=\kappa_2=1$ is the one found in $N=2$ supergravity (SUGRA), which is known to overcome the above-mentioned consistency problem.

TABLE I. List of parameters appearing in the loops and their numerical values.

g_A	H_A	h_A	f_π [MeV]	m_π [MeV]	M_N [MeV]	M_Δ [MeV]
1.27	2.28	2.85	92.4	139.6	939	1232

As the result, the $\gamma\Delta\Delta$ vertex becomes:

$$\Gamma^{\mu\nu\alpha}_{\gamma\Delta\Delta}(p',p) = eQ_\Delta\Big[-i\gamma^{\mu\nu\alpha} + i\frac{\kappa_1}{M_\Delta}(g^{\alpha\nu}q^\mu - g^{\alpha\mu}q^\nu) + \frac{\kappa_2}{M_\Delta}\varepsilon^{\mu\nu\rho\alpha}q_\rho\gamma_5\Big], \quad (15)$$

with $q = p' - p$, and denote $\kappa_{nm} \equiv \kappa_1 = \kappa_2$ in the resulting expressions of the Appendix. In this way by putting $\kappa_{nm} = 0$ or 1 we recover either the result of the minimal coupling or of the "truncated SUGRA". We want to note, that only the SUGRA choice ensures that the e.m. moments of the $\Delta(1232)$ take natural values at the tree level, see [23,51] for more details.

With the above and the notation in Appendix A, our results from the graphs in Fig. 1 for the isovector (V) nucleon anomalous magnetic moment κ_V and for the Dirac $\langle r_1^2\rangle_V$ and Pauli $\langle r_2^2\rangle_V$ radii are then:

$$\kappa_V = \frac{e}{2M_N}[\mathring{\kappa}_V + F_2^V(0)], \quad (16)$$

$$\langle r_1^2\rangle_V = \mathring{r}_V + 6\frac{d}{dq^2}\Big|_{q^2=0} F_1^V(q^2), \quad (17)$$

$$\langle r_2^2\rangle_V = \frac{6}{\kappa_V}\frac{d}{dq^2}\Big|_{q^2=0} F_2^V(q^2), \quad (18)$$

with

$$F_i^V(q^2) = [F_i^{N1}(q^2) + F_i^{N2}(q^2) + F_i^{N3}(q^2) + F_i^{N4}(q^2) + F_i^{N56}(q^2) + F_i^{N78}(q^2) + F_i^{NT12}(q^2)]^{p-n}. \quad (19)$$

We list all expressions for the $F_i^{Nj}(q^2)$ in Appendix B. The results for $N56$ and $NT2$ are not listed since they are independent of q^2 and contribute only to the nucleon charge which is renormalized. The $\mathring{\kappa}_V$ and the $\mathring{r}_V$ are the low energy constants (LECs) for the nucleon anomalous magnetic moment and the Dirac radius [52]. We fix these by constraining Eq. (16) and (17) to their phenomenological values at the physical pion mass: $\kappa_V = 3.7$ [53] and $\langle r_1^2\rangle_V = (0.765\ \text{fm})^2$ [9,54]. A LEC for the Pauli radius enters at a p^4 BχPT calculation. From an EFT viewpoint, the isovector and isoscalar nucleon combinations have a very different behavior. In the case of the isoscalar, unlike to the isovector part, sizeable two-loop corrections are known to appear [55]. We will not discuss the isoscalar quantities in our one-loop calculation.

Accordingly, our results from the graphs in Fig. 2 for the $\Delta^+(1232)$-isobar magnetic moment μ_Δ, electric quadrupole moment $\mathcal{Q}_\Delta$, magnetic octupole moment $\mathcal{O}_\Delta$ and the charge radius $\langle r_{E0}^2\rangle$ are:

$$\mu_\Delta = \frac{e}{2M_N}r[\mathring{\mu}_\Delta + F_2^\Delta(0)], \quad (20)$$

$$\mathcal{Q}_\Delta = \frac{e}{M_\Delta^2}\Big[\mathring{\mathcal{Q}}_\Delta - \frac{1}{2}F_3^\Delta(0)\Big], \quad (21)$$

$$\mathcal{O}_\Delta = \frac{e}{2M_\Delta^3}\Big[\mathring{\mathcal{O}}_\Delta + F_2^\Delta(0) - \frac{1}{2}(F_3^\Delta(0) + F_4^\Delta(0))\Big], \quad (22)$$

$$\langle r_{E0}^2\rangle = \mathring{r}_{E0} + 6\Big[\frac{d}{dq^2}\Big|_{q^2=0} F_1^\Delta(q^2) - \frac{1}{4M_\Delta^2}F_2^\Delta(0) - \frac{1}{12M_\Delta^2}F_3^\Delta(0)\Big], \quad (23)$$

with

$$F_i^\Delta(q^2) = [F_i^{\Delta 1}(q^2) + F_i^{\Delta 2}(q^2) + F_i^{\Delta 3}(q^2) + F_i^{\Delta 4}(q^2) + F_i^{\Delta 56}(q^2) + F_i^{\Delta 78}(q^2) + F_i^{\Delta T12}(q^2)]^{\Delta^+}. \quad (24)$$

All expressions for the $F_i^{\Delta j}(q^2)$ are given in Appendix C. The quantities $\mathring{\mu}_\Delta$, $\mathring{\mathcal{Q}}_\Delta$, $\mathring{\mathcal{O}}_\Delta$ and $\mathring{r}_{E0}$ are the LECs for the $\Delta^+(1232)$-isobar moments and its charge radius.

We estimate the error coming from terms higher order in m_π^2 by adding $\pm n\cdot m_\pi^2$ to our results where n is taken to be of *natural* size, i.e. $n = 1$.

In the upcoming sections we will use the following parameters for better reading:

$$\mu = \frac{m_\pi}{M_{sc}}, \qquad R = \frac{M_\Delta}{M_N}, \qquad r = \frac{M_N}{M_\Delta},$$
$$\tilde{q}^2 = \frac{q^2}{M_N^2}, \qquad \Delta = M_\Delta - M_N, \quad (25)$$

$$\delta = \frac{\Delta}{M_\Delta}, \qquad C_{NN} = \frac{g_A M_{sc}}{8f_\pi\pi},$$
$$C_{N\Delta} = \frac{h_A M_{sc}}{8f_\pi\pi}, \qquad C_{\Delta\Delta} = \frac{H_A M_{sc}}{8f_\pi\pi}, \quad (26)$$

where M_{sc} is the relevant mass scale for the observables in question, i.e. $M_{sc} = M_N$ for the nucleon quantities and $M_{sc} = M_\Delta$ for the $\Delta(1232)$ ones. We work in $d = 4 - 2\varepsilon$ dimensions.

C. Chiral structure and renormalization

As discussed in detail in Subsection II A, we employ the EOMS scheme [30] to renormalize the loops in Figs. 1 and 2. We cancel the ultraviolet divergences so that the renormalized LECs are equal to their "physical" values in the chiral limit. Within this renormalization prescription the divergences proportional to $L = -\frac{1}{\epsilon} + \gamma_E + \ln\frac{M_{sc}^2}{4\pi\Lambda^2}$ ($\tilde{M}S$ scheme), as well as the finite m_π constant terms, are absorbed into the corresponding LECs.

In App. B and C we give all nucleon and $\Delta(1232)$-isobar quantities renormalized with $\tilde{M}S$, the renormalization of the power-counting breaking terms is done in this section. We will see that all renormalized LECs will not change much by including various contributions.

For the nucleon isovector quantities to the order p^3 there are LECs for the Dirac radius and the anomalous magnetic

moment while one for the Pauli radius enters at the order p^4, cf. [52]. Schematically the chiral structures are:

$$\langle r_1^2\rangle_V = \mathring{r}_V + c_1 + \alpha_1 \ln\mu + \beta_1\mu + \mathcal{O}(\mu^2), \quad (27)$$

$$\kappa_V = \mathring{\kappa}_V + c_\kappa + \beta_\kappa\mu + \mathcal{O}(\mu^2), \quad (28)$$

$$\langle r_2^2\rangle_V = \gamma_2\frac{1}{\mu} + c_2 + \alpha_2 \ln\mu + \beta_2\mu + \mathcal{O}(\mu^2), \quad (29)$$

with c_i, α_i, β_i and γ_i as some definite constants given in the next section. In the chiral limit both radii diverge with $\ln\mu$ and $1/\mu$, respectively. The constants c_1 and c_κ have to be renormalized and are listed in Appendix B. In Table II we see how the values of the LECs $\mathring{r}_V$ and $\mathring{\kappa}_V$ change by renormalizing the above constants when taking into account: only virtual nucleons, virtual nucleons and $\Delta(1232)$ with minimal photon coupling, and virtual nucleons and $\Delta(1232)$ with truncated SUGRA. The renormalized values of the LECs do not change much by including the different contributions. Further, our results for the nucleon case are compatible to the p^4 calculation in [36].

In the case of the $\Delta(1232)$ electromagnetic quantities there are LECs for all multipole moments and the charge radius: $\mathring{\mu}_\Delta$, $\mathring{\mathcal{Q}}_\Delta$, $\mathring{\mathcal{O}}_\Delta$ and $\mathring{r}_{E0}$. Schematically the chiral structures are:

$$\mu_\Delta = \mathring{\mu}_\Delta + c_\mu + \beta_\mu\mu + \mathcal{O}(\mu^2), \quad (30)$$

$$\mathcal{Q}_\Delta = \mathring{\mathcal{Q}}_\Delta + c_\mathcal{Q} + \alpha_\mathcal{Q} \ln\mu + \beta_\mathcal{Q}\mu + \mathcal{O}(\mu^2), \quad (31)$$

$$\mathcal{O}_\Delta = \mathring{\mathcal{O}}_\Delta + c_\mathcal{O} + \beta_\mathcal{O}\mu + \mathcal{O}(\mu^2), \quad (32)$$

$$\langle r_{E0}^2\rangle = \mathring{r}_{E0} + c_r + \alpha_r \ln\mu + \beta_r\mu + \mathcal{O}(\mu^2). \quad (33)$$

TABLE II. Values of the LECs by considering various contributions to the observables. We use the following values for the nucleon isovector and $\Delta^+(1232)$ quantities at the physical point: $\langle r_1^2\rangle_V = 0.585$ fm^2, $\kappa_V = 3.7$, $\mu_\Delta = 2.7\mu_N$, $\mathcal{Q}_\Delta = -1.87\frac{e}{M_\Delta^2}$, $\mathcal{O}_\Delta = 0$ and $\langle r_{E0}^2\rangle = 0$. In the second column the N/Δ means to take only virtual nucleons ($\Delta(1232)$) contributions for the nucleon ($\Delta(1232)$) quantities, the third column to include both virtual baryons with minimal $\gamma\Delta\Delta$ coupling and the fourth to take the truncated SUGRA.

	N/Δ	$N+\Delta$ minimal	$N+\Delta$ nonminimal
$\mathring{r}_V$/fm^2	−0.69	−0.76	−0.74
$\mathring{\kappa}_V$	5.03	5.05	5.13
$\mathring{\mu}_\Delta/\mu_N$	2.78	2.73	2.87
$\mathring{\mathcal{Q}}_\Delta/\frac{e}{M_\Delta^2}$	−3.50	−3.49	−3.72
$\mathring{\mathcal{O}}_\Delta/\frac{e}{2M_\Delta^3}$	−0.40	−0.33	−0.12
$\mathring{r}_{E0}$/fm^2	−0.091	−0.086	−0.0831

In the chiral limit only the $\Delta(1232)$ EQM and its charge radius diverge with $\ln\mu$ whereas the MOM is finite. In the MOM the logarithm coming from the $F_3^\Delta(0)$ is exactly canceled by the same term appearing in $F_4^\Delta(0)$.

Again, the c_i have to be renormalized and are explicitly listed in the Appendix C. We use the following values for the physical point to see the changes of the LECs with respect to including the various contributions: $\mu_\Delta = 2.7\mu_N$, $\mathcal{Q}_\Delta = -1.87\frac{e}{M_\Delta^2}$. The $\Delta^+(1232)$ magnetic dipole moment is taken from [56] and the value for the quadrupole moment is a large N_c estimate, see Sec. IV B. For the octupole moment and the charge radius no information is available and we use: $\mathcal{O}_\Delta = 0$ and $\langle r_{E0}^2\rangle = 0$. The numbers for these quantities correspond to the bare change of the LECs.

In total we see that the renormalized LECs change within a reasonable degree.

III. RECOVERING THE HBχPT RESULTS

The nucleon electromagnetic quantities were studied within the $SU(2)$ heavy baryon χPT approach in Ref. [52] while the $\Delta(1232)$-isobar ones in the HBχPT $SU(3)$ calculation Ref. [33]. The HBχPT approach is an expansion in powers of $1/M_N$ where only the leading term is kept. We compare our covariant BχPT results with these studies and see that in this limit our formulas reduce to the HBχPT expressions. In Appendix B 1 we give our full results and discuss in this section only the terms up to the second order in m_π.

A. Nucleon electromagnetic form factors

To compare our results to the HBχPT study [52], we expand the HBχPT expression in m_π and Δ and absorb all constant terms into the LECs:

$$\langle r_1^2\rangle_V^{(\mathrm{HB})}\frac{1}{6} = \mathring{r}_V\frac{1}{6} - \frac{(1+5g_A^2)}{48f_\pi^2\pi^2}\ln\frac{m_\pi}{M_N} - \frac{m_\pi^2}{\Delta^2}\frac{5h_A^2}{864f_\pi^2\pi^2}\left(1+2\ln\frac{m_\pi}{2\Delta}\right), \quad (34)$$

$$\kappa_V^{(\mathrm{HB})} = \mathring{\kappa}_V - \frac{g_A^2M_Nm_\pi}{4f_\pi^2\pi} - \frac{h_A^2M_N}{72f_\pi^2\pi^2}\frac{m_\pi^2}{\Delta}\left(1-2\ln\frac{m_\pi}{2\Delta}\right), \quad (35)$$

$$\langle r_2^2\rangle_V^{(\mathrm{HB})}\frac{\kappa_V^{(\mathrm{HB})}}{6} = \frac{g_A^2M_N}{48f_\pi^2\pi m_\pi} - \frac{h_A^2M_N}{216f_\pi^2\pi^2\Delta}\ln\frac{m_\pi}{2\Delta} - \frac{h_A^2M_Nm_\pi^2}{864f_\pi^2\pi^2\Delta^3}\left(1+2\ln\frac{m_\pi}{2\Delta}\right). \quad (36)$$

We want to note that the Δ expansion is done only for the comparison purpose. The corresponding parts of our work with only nucleon contributions are:

$$\langle r_1^2\rangle_V^{(N)}\frac{1}{6}=\frac{\mathring{r}_V}{6}-\left(\frac{1+5g_A^2}{48f_\pi^2\pi^2}-\frac{11g_A^2m_\pi^2}{24f_\pi^2\pi^2M_N^2}\right)\ln\frac{m_\pi}{M_N}+\frac{35g_A^2m_\pi}{192f_\pi^2\pi M_N}-\frac{5g_A^2m_\pi^2}{192f_\pi^2\pi^2M_N^2}, \tag{37}$$

$$\kappa_V^{(N)}=\mathring{\kappa}_V-\frac{g_A^2M_Nm_\pi}{4f_\pi^2\pi}-\frac{g_A^2m_\pi^2}{8f_\pi^2\pi^2}-\frac{7g_A^2m_\pi^2}{8f_\pi^2\pi^2}\ln\frac{m_\pi}{M_N}, \tag{38}$$

$$\langle r_2^2\rangle_V^{(N)}\frac{\kappa_V}{6}=\frac{g_A^2M_N}{48f_\pi^2\pi m_\pi}+\frac{29g_A^2}{96f_\pi^2\pi^2}-\frac{35g_A^2m_\pi}{128f_\pi^2\pi M_N}+\frac{23g_A^2m_\pi^2}{288f_\pi^2\pi^2M_N^2}+\left(\frac{g_A^2}{4f_\pi^2\pi^2}-\frac{5g_A^2m_\pi^2}{8f_\pi^2\pi^2M_N^2}\right)\ln\frac{m_\pi}{M_N}. \tag{39}$$

The HBχPT results are reproduced and all additional terms are of higher order in $1/M_N$, however, some of these are numerically as important as the HBχPT expressions.

Expanding our expressions with $\Delta(1232)$ contributions and minimal $\gamma\Delta\Delta$ coupling in m_π gives:

$$\begin{aligned}\langle r_1^2\rangle_V^{(\Delta)}\frac{1}{6}=&\frac{m_\pi^2}{\Delta^2}\frac{C_{N\Delta}^2}{162R^4M_N^2}\Big(-30+50R-170R^2+243R^3-496R^4+991R^5-574R^6-254R^7+180R^8\\&+(96R^2-216R^3)\ln\frac{m_\pi}{M_N}+(-96R^2+192R^3-96R^4+240R^5+400R^6-2236R^7\\&+1328R^8+508R^9-360R^{10})\ln R+(40-25R+14R^2-107R^3+108R^4-60R^5\\&-100R^6+559R^7-332R^8-127R^9+90R^{10})\ln\frac{\Delta^2(R+1)^2}{M_N^2}\Big),\end{aligned} \tag{40}$$

$$\begin{aligned}\kappa_V^{(\Delta)}=&\frac{m_\pi^2}{\Delta M_N}\frac{C_{N\Delta}^2}{81R^4}\Big(-140+40R-328R^2+4R^3+12R^4+500R^5+56R^6-216R^7\\&+16R^5(45+20R-76R^2-7R^3+27R^4)\ln R+4(5+5R+26R^2-18R^3\\&-27R^4-45R^5-20R^6+76R^7+7R^8-27R^9)\ln\frac{\Delta^2(R+1)^2}{M_N^2}+144R^2\ln\frac{m_\pi}{M_N}\Big),\end{aligned} \tag{41}$$

$$\begin{aligned}\langle r_2^2\rangle_V^{(\Delta)}\frac{\kappa_V^{(\Delta)}}{6}=&\frac{M_N}{\Delta}\frac{C_{N\Delta}^2}{M_N^2486R^4}\Big(90-370R+451R^2+935R^3-1214R^4-78R^5+861R^6-807R^7-30R^8+162R^9\\&-12R^3(20+10R+210R^2-300R^3+52R^4+146R^5-148R^6-5R^7+27R^8)\ln R+3R(50-71R-179R^2\\&+242R^3+210R^4-300R^5+52R^6+146R^7-148R^8-5R^9+27R^{10})\ln\frac{\Delta^2(R+1)^2}{M_N^2}-144\ln\frac{m_\pi}{M_N}\Big)\\&+\frac{m_\pi^2M_N}{\Delta^3(1+R)}\frac{C_{N\Delta}^2}{M_N^2486R^4}\Big(40R-152R^2+582R^3-1912R^4+2540R^5+612R^6-4614R^7+2820R^8+660R^9\\&-648R^{10}+24R^3(-10-10R+50R^2+90R^3-337R^4+62R^5+412R^6-262R^7-55R^8+54R^9)\ln R\\&-6R(25-68R+32R^2-8R^3+43R^4+90R^5-337R^6+62R^7+412R^8-262R^9\\&-55R^{10}+54R^{11})\ln\frac{\Delta^2(R+1)^2}{M_N^2}+(-432R^2+1008R^3-1152R^4+432R^5)\ln\frac{m_\pi}{M_N}\Big).\end{aligned} \tag{42}$$

Expanding these expressions also in Δ yields the $\Delta(1232)$ contributions of Eqs. (34)–(36). Compared to the minimal $\gamma\Delta\Delta$ coupling, the nonminimal contributions give terms that are of higher $1/M_N$ order than those already present and do therefore not appear in a HBχPT calculation.

In total, our results reduce in the limit $M_N\to\infty$ to the corresponding HBχPT expressions of [52]. We also see explicitly that in the HBχPT numerical sizeable contributions, in that approach subleading in $1/M_N$, are dropped.

B. Δ(1232) electromagnetic form factors

In the case of the $\Delta(1232)$ em quantities, there exists the HBχPT $SU(3)$ calculation Ref. [33]. We will compare our covariant formulae with this nonrelativistic study.

To do that we expand our results of Appendix C to the second order in m_π below the $\Delta(1232)\to\pi N$ threshold:

$$\mu_\Delta \frac{1}{r} = \mathring{\mu}_\Delta + \frac{C_{\Delta\Delta}^2}{972}\Big(-288\mu\pi + \mu^2(-5440 + 7514\kappa_{nm} + (-2976 + 6864\kappa_{nm})\ln\mu)\Big)$$
$$+ \frac{C_{N\Delta}^2}{36(r-1)}(i\pi(6 + 12r - 18r^2 - 48r^3 + 24r^4 + 78r^5 - 18r^6 - 60r^7 + 6r^8 + 18r^9)$$
$$+ \mu^2(6 - 18r + 72r^3 - 72r^5 + i\pi(-12 - 48r^3 + 108r^5 - 72r^7) + 24\ln\mu$$
$$+ (96r^3 - 216r^5 + 144r^7)\ln r + (-6 - 24r^3 + 54r^5 - 36r^7)\ln(r^2-1)^2)), \tag{43}$$

$$\mathcal{Q}_\Delta = \mathring{\mathcal{Q}}_\Delta - \frac{C_{\Delta\Delta}^2}{486}\Big(-48\mu\pi + 192\ln\mu + \mu^2(-684 - 1794\kappa_{nm} + (3240 + 1872\kappa_{nm})\ln\mu)\Big)$$
$$- \frac{C_{N\Delta}^2}{18(r-1)^2}(i\pi(-6 + 6r + 14r^2 - 18r^3 - 8r^4 + 24r^5 - 8r^6 - 18r^7 + 14r^8 + 6r^9 - 6r^{10})$$
$$+ \mu^2(6 - 7r - 4r^2 + 25r^3 - 12r^4 - 30r^5 + 24r^6 + i\pi(4 - 6r + 8r^2 - 20r^3 + 40r^5 - 24r^6 - 30r^7 + 24r^8)$$
$$+ (-8 + 12r)\ln\mu + (-16r^2 + 40r^3 - 80r^5 + 48r^6 + 60r^7 - 48r^8)\ln r$$
$$+ (2 - 3r + 4r^2 - 10r^3 + 20r^5 - 12r^6 - 15r^7 + 12r^8)\ln(r^2-1)^2)), \tag{44}$$

$$\mathcal{O}_\Delta = \mathring{\mathcal{O}}_\Delta + \frac{C_{\Delta\Delta}^2}{2916}(-288\mu\pi + \mu^2(10168 - 2470\kappa_{nm} + (-27024 + 14352\kappa_{nm})\ln\mu))$$
$$+ \frac{C_{N\Delta}^2}{36(r^2-1)}(i\pi(-6 - 10r + 6r^2 + 18r^3 + 8r^4 + 6r^5 - 4r^6 - 26r^7 - 10r^8 + 12r^9 + 6r^{10})$$
$$+ \mu^2(-2 + 26r + 30r^2 + 10r^3 - 36r^5 - 24r^6 + i\pi(4 - 16r - 16r^2 + 24r^3 + 32r^4 + 28r^5$$
$$+ 12r^6 - 36r^7 - 24r^8) - 8\ln\mu + (32r + 32r^2 - 48r^3 - 64r^4 - 56r^5 - 24r^6 + 72r^7 + 48r^8)\ln r$$
$$+ (2 - 8r - 8r^2 + 12r^3 + 16r^4 + 14r^5 + 6r^6 - 18r^7 - 12r^8)\ln(r^2-1)^2)), \tag{45}$$

$$\langle r_{E0}^2\rangle = \mathring{r}_{E0} + 6\frac{C_{\Delta\Delta}^2}{81M_\Delta^2}\Big(-100 - \frac{144}{H_A^2}\Big)\ln\mu + 6\frac{C_{\Delta\Delta}^2}{1944M_D^2}(2760\mu\pi + \mu^2(16476 + 13680\ln\mu) + \kappa_{nm}\mu^2(13026 + 9360\ln\mu))$$
$$+ 6\frac{C_{N\Delta}^2}{72M_\Delta^2(r-1)^2}(i\pi(-48 + 54r + 116r^2 - 162r^3 - 80r^4 + 222r^5 - 56r^6 - 174r^7 + 128r^8 + 60r^9 - 60r^{10})$$
$$+ \mu^2(78 - 106r - 22r^2 + 214r^3 - 84r^4 - 300r^5 + 240r^6 + i\pi(4 - 24r + 80r^2 - 200r^3 + 364r^5$$
$$- 204r^6 - 300r^7 + 240r^8) + (-8 + 48r)\ln\mu + (-160r^2 + 400r^3 - 728r^5 + 408r^6 + 600r^7 - 480r^8)\ln r$$
$$+ (2 - 12r + 40r^2 - 100r^3 + 182r^5 - 102r^6 - 150r^7 + 120r^8)\ln(r^2-1)^2)), \tag{46}$$

where the factor r in μ_Δ comes from defining the quantity in μ_N and we included the factor $1/2$ for the $\mathcal{Q}_\Delta$ and the 6 for the $\langle r_{E0}^2\rangle$. We will now compare certain ratios of coefficients within our formulas against the same ratios extracted from [33].

Starting with $\langle r_{E0}^2\rangle$, the ratio between the $\Delta T1$ and $\Delta 1$ contribution of Fig. 2 in [33] is $25g_{\Delta\Delta}^2/81$ where it is in our work for the $\Delta^+(1232)$: $100H_A^2/144$. Together with the ratio of the $\Delta(1232)$ kinetic to interacting term of $2/3$ in our Lagrangian compared to the one used in [33], we obtain the same $\Delta T1/\Delta 1$ ratio. Further, our ratio of the μ term in μ_Δ to the $\ln\mu$ term in $\langle r_{E0}^2\rangle$ is $\frac{288}{972}/\frac{100}{81}$ which equals that of [33], i.e. $\frac{8}{27}/\frac{100}{81}$ where the factor 6 of the radius definition is not included in [33]. Comparing in this manner the formulas, we obtain an agreement for all coefficients of the various μ and $\ln\mu$ terms in the various moments and charge radius.

In total, we conclude that our formulas reduce in the limit of $M_N \to \infty$ to the HBχPT nonrelativistic ones. Comparing numerically several terms of our formulas against the leading $1/M_N$ parts show that sometimes sizeable contributions are dropped in HBχPT.

IV. COVARIANT BARYON χPT RESULTS

In this section we present our main results. We study the nucleon form factors at the physical point for small momentum transfer with respect to the extraction of the proton electric radius from experimental data. Further, we also study the chiral behavior of the nucleon and $\Delta(1232)$ form

factors for $Q^2 = 0$ with $m_\pi^2 < 0.3$ GeV^2 and compare them to available lattice QCD results.

A. Nucleon electromagnetic form factors

As discussed in the introduction the inclusion of pion-production effects in the interpolation of low-Q^2 data for the proton electric form factor can be addressed within the framework of the baryon χPT. It is the second derivative of $G_E^p(q^2)$ which is a genuine prediction of this theory and constrains the analytic structure of the form factor at small spacelike momentum transfers, $-q^2 \leq 0.01$ GeV^2. Including such constraints in the proton charge radius extraction from electron-scattering data could have a quantitative impact.

The proton electric form factor expanded to second order in q^2 is:

$$G_E^p(q^2) = F_1^p(q^2) + \frac{q^2}{4M_N^2} F_2^p(q^2) = 1 + q^2 \frac{\langle r_E^2 \rangle_p}{6} + \frac{1}{2} q^4 \frac{d^2}{[dq^2]^2} G_E^p(0) + \mathcal{O}(q^6), \quad (47)$$

where we obtain for $\frac{d^2}{[dq^2]^2} G_E^p(0)$ from App. B 1 the following result at the physical point:

$$\frac{d^2}{[dq^2]^2} G_E(0) \cdot \text{GeV}^4 = 2.089 I_{N1} - 0.001 I_{N2} + 0.640 I_{NT1} + 0.580 I_{N3} - 0.021 I_{N4} + \kappa_{nm} 1.797 I_{N4}, \quad (48)$$

with I_i as the isospin factors. Since the important contributions, apart from the truncated SUGRA, come from the diagrams N1, NT1 and N3, we can make a direct comparison to the HBχPT results of Ref. [52]:

$$\frac{d^2}{[dq^2]^2} G_E^{p(\text{HB})}(0) = \frac{1 + 7g_A^2}{960 f_\pi^2 m_\pi^2 \pi^2} - g_{PND}^2 \times \frac{7(m_\pi^2 - \Delta^2 + \Delta\sqrt{-m_\pi^2 + \Delta^2} \ln \frac{\Delta + \sqrt{-m_\pi^2 + \Delta^2}}{m_\pi})}{1080 f_\pi^2 \pi^2 (m_\pi^2 - \Delta^2)^2}. \quad (49)$$

The first term comes from the diagrams N1, NT1 and is also the $1/M_N$ leading term in our results. Expanding our results in Δ coincides with the leading $1/M_N$ part of the same expansion in the HBχPT.

In Table III we compare our covariant numbers with those of the HBχPT. These numbers are to be entered for $\frac{d^2}{[dq^2]^2} G_E^p(0)$ in Eq. (47). In the case of only virtual nucleons, second column, the difference of the results are the additional terms of higher $1/M_N$ orders in the diagram N1. In HBχPT the second derivative is dominated by $\frac{d^2}{[dq^2]^2} F_1^p(0)$ where the contributions coming from $\frac{d}{dq^2} F_2^p(0)$ are of subleading order. However, these terms are in case of the $\Delta(1232)$ contributions, third column, the main cause of the difference. The nonminimal $\gamma\Delta\Delta$ coupling contributions are not present in the HBχPT. The large number comes from the m_π-constant terms in $\frac{d^2}{[dq^2]^2} F_1^p(0)$ and $\frac{d}{dq^2} F_2^p(0)$. These terms are of the same size as the corresponding constant appearing in the Pauli radius by considering only nucleons, Eq. (39), and are also discussed with respect to the chiral behavior later. Using the numbers of Table III to constrain the extrapolation of experimental data in the region of $Q^2 \leq 0.01$ GeV^2 could have a quantitative impact on the extracted number for $\langle r_E^2 \rangle_p$.

Another application of our BχPT form factor results is to study their chiral behavior in comparison to lattice QCD calculations. In Fig. 3 we show the nucleon isovector quantities κ_V, $\langle r_1^2 \rangle_V$ and $\langle r_2^2 \rangle_V$. The red solid curve corresponds to taking all contributions, truncated SUGRA, while the blue long-dashed curve to taking virtual baryons with strictly minimal photon couplings. The green short-dashed curve corresponds to the calculation with only virutal nucleons. The lQCD results are those of the LHPC collaboration [17,20], of the work [18] and of the QCDSF/UKQCD collaboration [19]. In our p^3 BχPT calculation appear LECs for the quantities κ_V and $\langle r_1^2 \rangle_V$ and we constrain our results to the experimental values: $\kappa_V = 3.7$ [53] and $\langle r_1^2 \rangle_V = 0.585$ fm^2 [9,54].

For the isovector anomalous magnetic moment κ_V and the Dirac radius $\langle r_1^2 \rangle_V$, we see that the lQCD and our BχPT results agree within the χPT error for pion masses above $m_\pi^2 = 0.1$ GeV^2. However, the data points for the smaller pion masses are not reached. A similar behavior is found in [17–19]. In these works the LHPC results were tried to fit by a HBχPT small scale expansion calculation with inclusion of explicit $\Delta(1232)$-isobar and a covariant NNLO BχPT without explicit $\Delta(1232)$-isobar. Conclusions in [17,19] are that the lattice LHPC data could not be fitted simultaneously.

In the case of the Pauli radius $\langle r_2^2 \rangle_V$ to the order p^3 there appears no LEC, hence the results are predictions. A LEC enters at the order p^4. We see that our truncated SUGRA

TABLE III. Contributions to the second derivative of the proton electric charge radius, $\frac{d^2}{[dq^2]^2} G_E^p(0)$, from the covariant baryon χPT in units of GeV^{-4}. The columns correspond to: second one to taking only virtual nucleons, third one to taking only virtual $\Delta(1232)$ with minimal $\gamma\Delta\Delta$ coupling, fourth to the truncated SUGRA and last one to the sum of all contributions.

Diagrams	N1 + N2 + NT1	N3 + N4	N4 nm	Sum
Covariant BχPT	4.80	−0.45	4.79	9.14
HBχPT	7.83	−1.30	−−	6.53

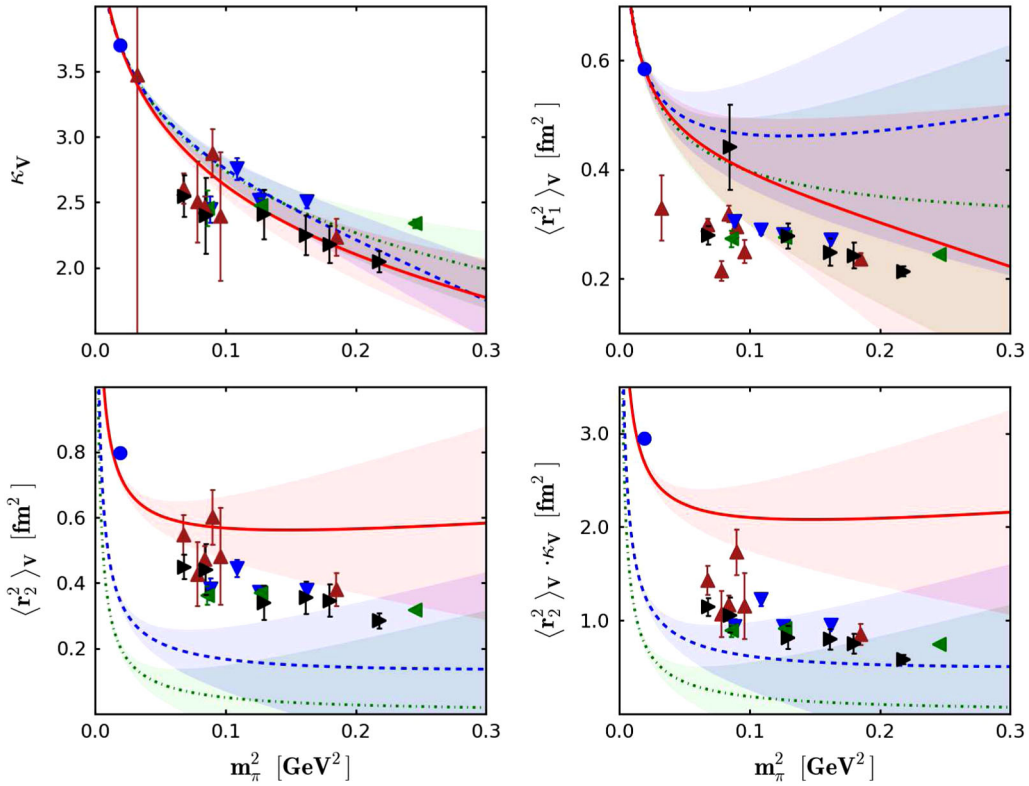

FIG. 3 (color online). Nucleon isovector anomalous magnetic moment κ_V and the Dirac $\langle r_1^2\rangle_V$ and Pauli $\langle r_2^2\rangle_V$ radii. The results correspond to: solid (red) curve to nucleon and $\Delta(1232)$ contributions with truncated SUGRA; long-dashed (blue) curve to our result with virtual nucleons and $\Delta(1232)$ with minimal coupling; short-dashed (green) curve to only virtual nucleon. The lattice results are taken from: blue down-triangles [17], black right-triangles [18], brown up-triangles [19], green left-triangles [20]. The blue circles denote the phenomenological values.

results nearly hits the experimental value. The reason is the m_π-constant contribution from the nonminimal $\gamma\Delta\Delta$ coupling. This term is of the same size as the constant $\frac{29g_A^2}{96f_\pi^2\pi^2}$ coming from the usual virtual nucleon contribution, Eq. (39). However there, the two negative m_π terms are the cause of the small BχPT result with only nucleons. The whole m_π dependence of $\langle r_2\rangle_V^2$ coming from all considered diagrams is dominated by the nucleon diagrams $N1$ and $N2$. The $\Delta(1232)$ contributions add merely a small constant term in the case of minimal photon coupling and a large term for the nonminimal coupling. In a p^4 calculation these parts would be renormalized.

For the Pauli-radius, our BχPT study and the lQCD results have the fact in common that the m_π^2 dependence is nearly linear for pion masses $m_\pi^2 \gtrsim 0.1$ GeV^2. However, the absolute values of $\langle r_2^2\rangle_V$ are rather different indicating that some unknown components in the BχPT or lQCD calculations are missing.

In this and other works finite volume lQCD results are compared to infinite volume BχPT ones. Finite volume effects on the BχPT side are known to be missing and could be one part of the explanation for the above discrepancies, especially for the small pion mass region. Further studies are presently done in that direction.

B. $\Delta(1232)$ electromagnetic form factors

We now proceed to the $\Delta^+(1232)$-isobar magnetic dipole (MDM), μ_{Δ^+}, electric quadrupole (EQM), $\mathcal{Q}_{\Delta^+}$, magnetic octupole (MOM), $\mathcal{O}_{\Delta^+}$, moments and its charge radius (CR), $\langle r_{E0}^2\rangle$. The experimental knowledge of the $\Delta^+(1232)$-isobar is rather scarce. For the $\Delta^+(1232)$-isobar MDM a value is obtained from the radiative pion photoproduction $\gamma N \to \pi N\gamma'$ [56]:

$$\mu_{\Delta^+} = 2.7^{+1.0}_{-1.3}(\text{stat.}) \pm 1.5(\text{syst.}) \pm 3.9(\text{theor.}). \quad (50)$$

For the $\Delta^+(1232)$ EQM we use the following model-independent estimation based on the large-N_c limit. In Ref. [57] the large-N_c relation $\mathcal{Q}_{\Delta^+} = \frac{2\sqrt{2}}{5}\mathcal{Q}_{p\Delta} + \mathcal{O}(N_c^{-2})$ was found which, combined with the $\Delta(1232)$-nucleon electric quadrupole moment of $\mathcal{Q}_{p\Delta} = (-0.0846 \pm 0.0033)\ e\,\text{fm}^2$ [58], gives a $\Delta^+(1232)$-isobar EQM estimation at the physical pion mass of:

$$\mathcal{Q}_{\Delta^+} = (-0.048 \pm 0.002)\ e\,\text{fm}^2 \approx -1.87\frac{e}{M_\Delta^2}. \quad (51)$$

Both values for μ_{Δ^+} and $\mathcal{Q}_{\Delta^+}$ are represented by blue circles in Fig. 4. There is no experimental knowledge on the $\Delta(1232)$-isobar MOM and CR. The Fig. 4 shows our results for the $\Delta(1232)$-isobar electromagnetic quantities

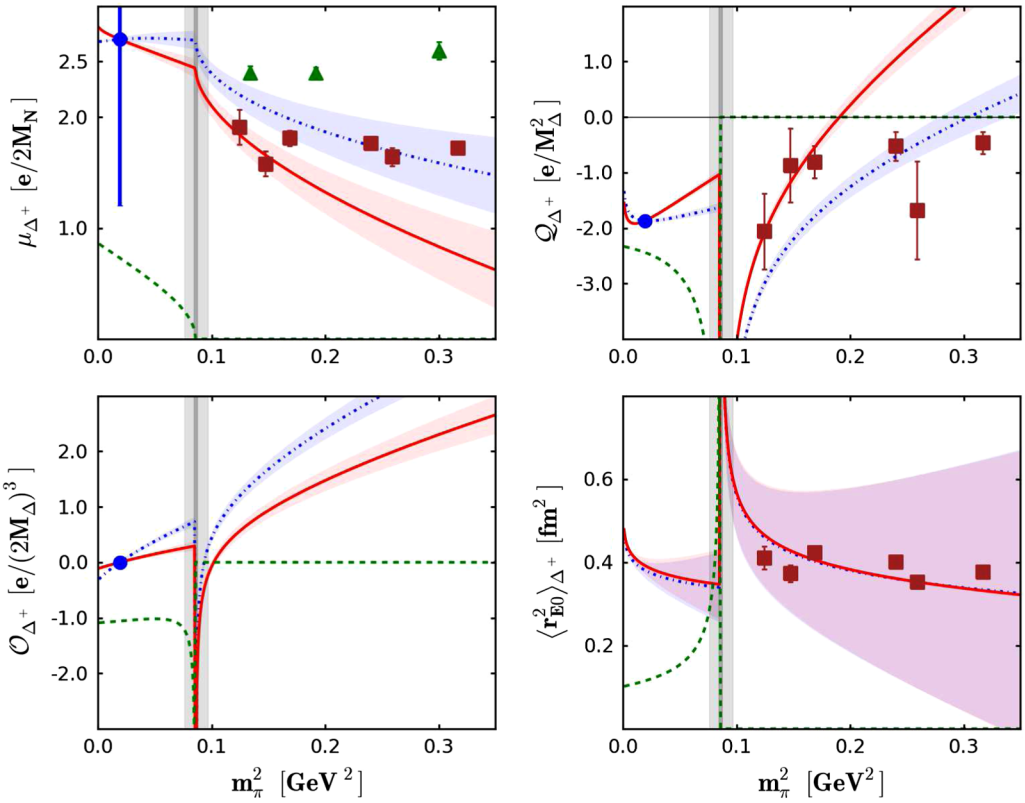

FIG. 4 (color online). The magnetic dipole MDM, electric quadrupole EQM, magnetic octupole MOM moments of the $\Delta^+(1232)$ and its charge radius CR. Both the results for the real part are shown with (red solid curves) and without (blue dashed curves) inclusion of the $\gamma\Delta\Delta$ nonminimal coupling, respectively. The green short-dashed curves depict the imaginary parts of these quantities. The blue circle correspond to the experimental value $\mu_{\Delta^+} = (2.7 \pm 1.5)\mu_N$, a large-$N_c$ estimation $\mathcal{Q}_{\Delta^+} = -1.87\frac{e}{M_\Delta^2}$ and $\mathcal{O}_{\Delta^+} = 0$. The lQCD data of [21] are denoted by green triangles while those of [22] are depicted by orange rectangles. The grey bands are described in the text.

compared to the lQCD results of [21,22]. The red solid curves correspond to the real parts with truncated SUGRA while the blue long-dashed curves correspond to excluding the nonminimal couplings. The green short-dashed curve are the imaginary parts which vanishes above $m_\pi = M_\Delta - M_N$. The lQCD studies apply different extraction techniques for the $\Delta^+(1232)$-isobar electromagnetic moments. The Ref. [21] extracted the MDM by applying the external background field technique while in [22] the MDM, EQM and CR are obtained through the form factors evaluated at finite Q^2 and extrapolating to $Q^2 = 0$ by dipole and exponential fits.

There are two pion mass regions for the $\Delta(1232)$-isobar. Above the threshold $m_\pi = M_\Delta - M_N$ the $\Delta(1232)$ is stable while below the $N\pi$ decay channel is open. Striking features in Fig. 4 are the cusp and singularities in the real and imaginary parts of the moments and CR at this pion mass. They result from the fact that resonance electromagnetic properties at and near the opening of thresholds are not well-defined [59].

The MDM μ, taken as the example, is usually defined by the linear energy shift of the particle in an external magnetic field $\vec{B}$:

$$M(\vec{B}) = M_0 - \vec{\mu} \cdot \vec{B} + O(B^2). \tag{52}$$

However, the energy change of unstable particles depend nonanalytically on $\vec{B}$ and the above linear approximation can only be used when the following condition is met [59]:

$$\frac{e|\vec{B}|}{2M_\Delta|M_\Delta - M_N - m_\pi|} \ll 1. \tag{53}$$

At the pion mass $m_\pi = M_\Delta - M_N$ this is not the case and as a consequence the conventionally used one-photon approximation to extract a the moment is not valid. Moreover, for a given magnetic field strength $|\vec{B}|$, there exists a pion mass region for which the $\Delta^+(1232)$-isobar energy is not accurately approximated by Eq. (52), i.e. where the MDM is not well defined. This is directly relevant for lattice QCD investigations where the periodic boundary conditions limit the values of $|\vec{B}|$.

To give explicit situations, we take two examples. Once a spatial lattice of $L = 32$ with spacing $a^{-1} = 1$ GeV and once $L = 24$ with $a^{-1} = 2$ GeV. We compare the magnetic field implementation by $eBa^2 = 2\pi/L$ as in Ref. [60] and by $eBa^2 = 2\pi/L^2$ as in [21]. Further, we take Eq. (53) to be unity, i.e. a completely nonfulfillment of this relation,

and solve for the region around the threshold $m_\pi = M_\Delta - M_N$. Within this region higher order $\vec{B}$ contributions can not be neglected. For the finer lattice and linear-L implementation this region is $m_\pi = 213.4$–372.6 MeV and for the quadratic-L case $m_\pi = 290.5$–295.5 MeV. For the second setting the regions are for the linear-L $m_\pi = -131.8$–717.8 MeV and for the quadratic-L $m_\pi = 275.3$–310.7 MeV. We represent the two regions for the quadratic-L implementation as grey bands in Fig. 4.

The above considerations are directly applicable to the extraction of $\Delta(1232)$-isobar moments by the external background field method as used, e.g., in [21]. The Eq. (53) gives a relation on how to chose the parameters in order to interpret the extracted lQCD number as a MDM. We like to notice that the work [21] uses pion masses where Eq. (53) is not violated. However, future lattices will soon allow for pion masses where this will be the case.

The implications of the cusp and singularities on the three-point function method is more subtle. Form factors data points are obtained for finite Q^2 and extrapolated by dipole or exponential fits to $Q^2 = 0$. In the present case the cusp and singularities fall on $Q^2 = 0$ for $m_\pi = M_\Delta - M_N$. Qualitatively, a finite Q^2 would enter as an additional energy parameter and the singularities would shift to $Q^2 \neq 0$ related to $m_\pi \neq M_\Delta - M_N$. For lattice calculations this could mean that one extrapolates across this singularity when all data points are on the right of the singularity.

Apart from the cusp and singularities we see that the present BχPT study seems to be consistent with the lQCD data. With respect to the phenomenological uncertainties of the values at $m_\pi = 139$ MeV, we can adjust the LECs $\mathring{\mu}_\Delta$, $\mathring{\mathcal{Q}}_\Delta$, $\mathring{\mathcal{O}}_\Delta$ and $\mathring{r}_{E0}$ such that both our results could agree with both lQCD works [21,22]. Further, the rather small physical $\Delta(1232)$ electric radius, ~ 0.39 fm^2, was also reported in the works [39,61].

In the chiral limit the EQM and the CR are logarithmically divergent while the MDM and MOM are finite. In the case of the MOM the divergent part of $F_2(q^2)$ is canceled by an equally divergent part in $F_4(q^2)$.

V. HIGHER-ORDER EFFECTS

In this section we investigate the "robustness" of our results by including several contributions which are nominally of higher order. One such effect is the pion-mass dependence of the LECs, such as g_A, f_π, M_N and M_Δ. In the above we have taken them to be at the physical pion mass, whereas the Lagrangian is expressed in terms of their chiral-limit values. The difference between the two is usually of order p^2, and since our leading result is of order p^3, the effect of varying these LECs with the pion mass should be of order p^5. As we have not even included the p^4 contributions, the consideration of the p^5 effects seems premature. However, there are at least two reasons for doing it here. First, as an error estimate according to Beane [62]. The second reason is due to the fact that the position of the cut associated with the decay of the Δ depends on the Δ-nucleon mass difference, and hence the small variations in this parameter may potentially lead to significant effects in the quantities that are singular at the decay threshold.

In Fig. 5, we investigate the nucleon and $\Delta(1232)$ magnetic moments with variation of f_π and the baryon masses, according to the following formulae [15,46]:

$$f_\pi(m_\pi^2) = \mathring{f}_\pi\left(1 - \frac{m_\pi^2}{16\pi^2 \mathring{f}_\pi^2} \ln\frac{m_\pi^2}{\Lambda^2}\right), \tag{54}$$

$$M_N(m_\pi^2) = \mathring{M}_N - 4c_{1N}m_\pi^2 + \Sigma_N(m_\pi^2), \tag{55}$$

$$M_\Delta(m_\pi^2) = \mathring{M}_\Delta - 4c_{1\Delta}m_\pi^2 + \mathrm{Re}\Sigma_\Delta(m_\pi^2), \tag{56}$$

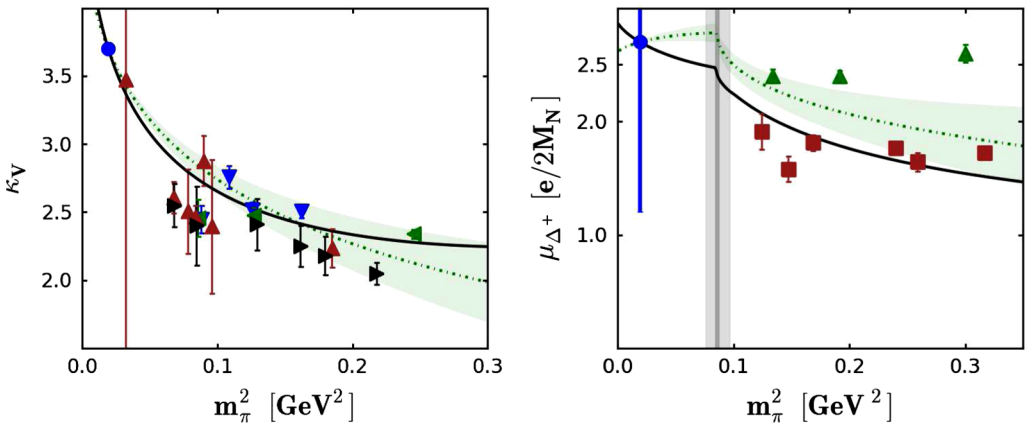

FIG. 5 (color online). Chiral behavior of the nucleon and $\Delta(1232)$ magnetic moments with πN loops. We compare our results obtained with the phenomenological values for the coupling constants and baryon masses, green dashed line, against those with including also the pion mass dependence of f_π, M_N and M_Δ, solid black line. The lattice data are the same as in Figs. 3 and 4.

with $\mathring{f}_\pi = 87$ MeV, $\mathring{M}_N = 883$ MeV, $c_{1N} = -0.87$ GeV^{-1}, $\mathring{M}_\Delta = 1200$ MeV, $c_{1\Delta} = -0.40$ GeV^{-1} and the Σ_N, Σ_Δ given in Appendix D. We do not include the pion mass dependence of the axial-vector constants since their chiral behavior is not well constrained [62] and seems to be not as prominent as those of f_π, M_N and M_Δ [63].

In the left panel we can see that the variation of f_π and M_N with m_π in the leading-order expressions for the nucleon a.m.m. results in the transition from the dashed to the solid line. The effect is within the error band, but curvature has appreciably increased which helps to connect the lattice data with experiment.

In the right panel the variation of f_π, M_N and M_Δ in the expressions for the πN-loop contribution to the magnetic moment of the Δ results in the transition from the dashed to the solid line. Again, the effect is appreciable but nonetheless is within the error with respect to the inclusion of virtual $\Delta(1232)$, Fig. 4. The cusp appears at a nearly the same position, i.e., is shifted by several MeV due to the small change in the Delta-nucleon mass difference.

VI. SUMMARY AND CONCLUSION

We have investigated the electromagnetic moments, radii, and form factors of the nucleon and $\Delta(1232)$ baryons in the realm of chiral perturbation theory. Analyticity (microcausality) is playing an important role in these quantities, and hence, in contrast to previous investigations, we have performed the calculations in the EOMS scheme. We have obtained analytical expressions for various contributions to the nucleon isovector magnetic moments, Dirac- and Pauli-radius as well as the $\Delta(1232)$-isobar magnetic dipole, electric quadrupole and magnetic octupole moments and charge radius, and compared the results to experimental data and to recent lattice QCD calculations where available.

BχPT predicts the analytic structure of the form factors at small Q^2 and can serve the purpose of extrapolating the electron-scattering data to $Q^2 = 0$. We calculated the value of the second derivative of the proton electric form factor $G_E^p(q^2)$ in BχPT.

We have analyzed the cusps and singularities appearing in the pion mass dependence of the $\Delta(1232)$ electromagnetic quantities at the point where the $\Delta \to N\pi$ decay channel opens. These singularities are connected to the fact that em properties of unstable particles at the threshold are not well defined in perturbation theory. The self-energy of unstable particles depend on the external magnetic field in a essentially nonanalytic fashion. This has an impact on the extraction of lQCD em moments of unstable particles near their decay threshold. To interpret the number extracted in lQCD in the vicinity of the opening of decay channels as an em moment, the applied external magnetic field or the Q^2 data points of the form factor have to be chosen specifically.

Comparing the chiral behavior of the nucleon em quantities given by our covariant BχPT to recent lQCD studies, we see that our results for the isovector anomalous magnetic moment and Dirac radius are in qualitative agreement (within the BχPT uncertainties) with lQCD results for $m_\pi^2 > 0.1$ GeV^2. Including finite volume effects in our BχPT formulae is the next step and expected to resolve some of the discrepancies in the $m_\pi^2 < 0.1$ GeV^2 region.

ACKNOWLEDGMENTS

The work of T. L was partially supported by the Research Centre Elementarkraefte und Mathematische Grundlagen at the Johannes Gutenberg University Mainz. J. M. C acknowledges the MEC contract FIS2006-03438, the EU Integrated Infrastructure Initiative Hadron Physics Project contract RII3-CT-2004-506078 and the Science and Technology Facilities Council Grant No. ST/H004661/1 for support.

APPENDIX A: NOTATIONS

1. Form factors

The e.m. form factors are defined through the Lorentz decomposition of the matrix element of the vector current, $V^\mu = \bar{\Psi}(0)\gamma^\mu\Psi(0)$, between baryon states. In the case of the nucleon,

$$\langle N(p')|\bar{\Psi}(0)\gamma^\mu\Psi(0)|N(p)\rangle = \bar{u}(p')\left[\gamma^\mu F_1^N(Q^2) + \frac{i\sigma^{\mu\nu}q_\nu}{2M_N}F_2^N(Q^2)\right]u(p), \quad \text{(A1)}$$

with $q = p' - p$, $Q^2 = -q^2$, and $u(p)$ as the nucleon spinor with mass M_N. The invariants F_1 and F_2 are the Dirac and Pauli form factors, respectively, which at $Q^2 = 0$ yield the nucleon charge in units of e and the nucleon anomalous magnetic moment:

$$F_1^N(0) = e_N, \qquad F_2^N(0) = \kappa_N. \quad \text{(A2)}$$

One distinguishes the isovector and isoscalar nucleon form factors as:

$$F_i^V(Q^2) = F_i^p(Q^2) - F_i^n(Q^2),$$
$$F_i^S(Q^2) = F_i^p(Q^2) + F_i^n(Q^2). \quad \text{(A3)}$$

In the case of the $\Delta(1232)$, which has spin $3/2$, there are four independent form factors:

$$\langle\Delta(p')|V^\mu|\Delta(p)\rangle = -\bar{u}_\alpha(p')\left\{\left[F_1^\Delta(Q^2)\gamma^\mu + \frac{i\sigma^{\mu\nu}q_\nu}{2M_\Delta}F_2^\Delta(Q^2)\right]g^{\alpha\beta} + \left[F_3^\Delta(Q^2)\gamma^\mu + \frac{i\sigma^{\mu\nu}q_\nu}{2M_\Delta}F_4^\Delta(Q^2)\right]\frac{q^\alpha q^\beta}{4M_\Delta^2}\right\}u_\beta(p), \quad \text{(A4)}$$

where $u_\alpha(p)$ is a Rarita-Schwinger spinor for the spin-3/2 $\Delta(1232)$-isobar state of mass M_Δ. The multipole form factors G_{E0}, G_{M1}, G_{E2}, G_{M3} of the Δ are expressed in terms of F's as follows:

$$
\begin{aligned}
G_{E0}(Q^2) &= F_1^\Delta(Q^2) - \tau F_2^\Delta(Q^2) + \frac{2}{3}\tau G_{E2}(Q^2),\\
G_{E2}(Q^2) &= F_1^\Delta(Q^2) - \tau F_2^\Delta(Q^2)\\
&\quad - \frac{1}{2}(1+\tau)[F_3^\Delta(Q^2) - \tau F_4^\Delta(Q^2)],\\
G_{M1}(Q^2) &= F_1^\Delta(Q^2) + F_2^\Delta(Q^2) + \frac{4}{5}\tau G_{M3}(Q^2),\\
G_{M3}(Q^2) &= F_1^\Delta(Q^2) + F_2^\Delta(Q^2)\\
&\quad - \frac{1}{2}(1+\tau)[F_3^\Delta(Q^2) + F_4^\Delta(Q^2)],
\end{aligned}
\tag{A5}
$$

with $\tau = Q^2/(4M_\Delta^2)$. At $Q^2 = 0$, the multipole form factors define the static moments: charge e_Δ, magnetic dipole moment μ_Δ, electric quadrupole moment $\mathcal{Q}_\Delta$ magnetic octupole moment $\mathcal{O}_\Delta$, i.e.:

$$
\begin{aligned}
e_\Delta &= G_{E0}(0) = F_1^\Delta(0),\\
\mu_\Delta &= \frac{e}{2M_\Delta} G_{M1}(0) = \frac{e}{2M_\Delta}[e_\Delta + F_2^\Delta(0)],\\
\mathcal{Q}_\Delta &= \frac{e}{M_\Delta^2} G_{E2}(0) = \frac{e}{M_\Delta^2}\left[e_\Delta - \frac{1}{2}F_3^\Delta(0)\right],\\
\mathcal{O}_\Delta &= \frac{e}{2M_\Delta^3} G_{M3}(0)\\
&= \frac{e}{2M_\Delta^3}\left[e_\Delta + F_2^\Delta(0) - \frac{1}{2}(F_3^\Delta(0) + F_4^\Delta(0))\right].
\end{aligned}
\tag{A6}
$$

Besides the static moments, the slopes of the form factors are of interest as they indicate the radii of the respective e.m. distributions; generically:

$$
\langle r^2 \rangle = \frac{6}{F(0)} \frac{dF(q^2)}{dq^2} \tag{A7}
$$

2. Isospin and Lorentz structures

The isospin 1/2 to 3/2 and 3/2 to 3/2 transition matrices T^a and $\mathcal{T}^a$ appearing in the $N\Delta$ and $\Delta\Delta$ Lagrangians are given by:

$$
T^1 = \frac{1}{\sqrt{6}}\begin{pmatrix} -\sqrt{3} & 0 & 1 & 0 \\ 0 & -1 & 0 & \sqrt{3} \end{pmatrix} \qquad \mathcal{T}^1 = \frac{2}{3}\begin{pmatrix} 0 & \frac{\sqrt{3}}{2} & 0 & 0 \\ \frac{\sqrt{3}}{2} & 0 & 1 & 0 \\ 0 & 1 & 0 & \frac{\sqrt{3}}{2} \\ 0 & 0 & \frac{\sqrt{3}}{2} & 0 \end{pmatrix} = \mathcal{T}^{1\dagger} \qquad T^2 = \frac{-i}{\sqrt{6}}\begin{pmatrix} \sqrt{3} & 0 & 1 & 0 \\ 0 & 1 & 0 & \sqrt{3} \end{pmatrix}
$$

$$
\mathcal{T}^2 = \frac{2i}{3}\begin{pmatrix} 0 & -\frac{\sqrt{3}}{2} & 0 & 0 \\ \frac{\sqrt{3}}{2} & 0 & -1 & 0 \\ 0 & 1 & 0 & -\frac{\sqrt{3}}{2} \\ 0 & 0 & \frac{\sqrt{3}}{2} & 0 \end{pmatrix} = \mathcal{T}^{2\dagger} \qquad T^3 = \sqrt{\frac{2}{3}}\begin{pmatrix} 0 & 1 & 0 & 0 \\ 0 & 0 & 1 & 0 \end{pmatrix} \qquad \mathcal{T}^3 = \begin{pmatrix} 1 & 0 & 0 & 0 \\ 0 & 1/3 & 0 & 0 \\ 0 & 0 & -1/3 & 0 \\ 0 & 0 & 0 & -1 \end{pmatrix} = \mathcal{T}^{3\dagger}
$$

$$
Q_\pi^{ab} = -i\varepsilon^{ab3} \qquad Q_N = \frac{1}{2}(1+\tau^3) \qquad Q_{N\Delta} = \frac{1}{2}(1+3\mathcal{T}^3) \qquad Q_\Delta = \frac{1}{2}(1+3\mathcal{T}^3). \tag{A8}
$$

The totally antisymmetric Dirac matrices products appearing in the $N\Delta$ and $\Delta\Delta$ Lagrangians are defined as:

$$
\gamma^{\mu\nu} = \frac{1}{2}[\gamma^\mu, \gamma^\nu], \qquad \gamma^{\mu\nu\rho} = \frac{1}{2}\{\gamma^{\mu\nu}, \gamma^\rho\} = -i\varepsilon^{\mu\nu\rho\sigma}\gamma_\sigma\gamma_5, \qquad \gamma^{\mu\nu\rho\sigma} = \frac{1}{2}[\gamma^{\mu\nu\rho}, \gamma^\sigma] = i\varepsilon^{\mu\nu\rho\sigma}\gamma_5, \tag{A9}
$$

with the convention: $\varepsilon_{0123} = -\varepsilon^{0123} = +1$.

3. Loop integrals

In this work the following loop integrals appear:

$$
\begin{aligned}
J_n(\mathcal{M}) &= \int \frac{d^dl}{(2\pi)^d} \frac{1}{[l^2 - \mathcal{M}]^n} = \frac{i}{(4\pi)^{d/2}}(-1)^n \frac{\Gamma(n - \frac{d}{2})}{\Gamma(n)}[\mathcal{M}]^{(d/2)-n}\\
&\int \frac{d^dl}{(2\pi)^d} \frac{l_\kappa l_\lambda}{[l^2 - \mathcal{M}]^n} = \frac{1}{2(n-1)} J_{n-1}(\mathcal{M}) g_{\kappa\lambda}\\
&\int \frac{d^dl}{(2\pi)^d} \frac{l_\alpha l_\beta l_\mu l_\nu}{[l^2 - \mathcal{M}]^n} = \frac{g_{\alpha\beta}g_{\mu\nu} + g_{\beta\mu}g_{\alpha\nu} + g_{\beta\nu}g_{\alpha\mu}}{4(n-1)(n-2)} J_{n-2}(\mathcal{M}).
\end{aligned}
\tag{A10}
$$

The corresponding solutions are:

$$J_1(\mathcal{M}) = \frac{-i}{(4\pi)^2} M_{sc}^2 \tilde{\mathcal{M}}[L - 1 + \ln\tilde{\mathcal{M}}]$$
$$J_2(\mathcal{M}) = \frac{-i}{(4\pi)^2}[L + \ln\tilde{\mathcal{M}}]$$
$$J_3(\mathcal{M}) = \frac{-i}{(4\pi)^2}\frac{1}{2M_{sc}^2}\frac{1}{\tilde{\mathcal{M}}}, \tag{A11}$$

with $\tilde{\mathcal{M}} = \mathcal{M}/M_{sc}^2$, where M_{sc} is the relevant mass scale, and $L = -\frac{1}{\epsilon} + \gamma_E + \ln\frac{M_{sc}^2}{4\pi\Lambda^2}$. We work in $d = 4 - 2\epsilon$ dimensions.

The D-dimensional spin-3/2 Δ-isobar propagator is given by:

$$S_\Delta^{\alpha\beta}(p) = \frac{\not{p} + M_\Delta}{p^2 - M_\Delta^2 + i\varepsilon}\Big[-g^{\alpha\beta} + \frac{1}{D-1}\gamma^\alpha\gamma^\beta + \frac{1}{(D-1)M_\Delta}(\gamma^\alpha p^\beta - \gamma^\beta p^\alpha) + \frac{D-2}{(D-1)M_\Delta^2}p^\alpha p^\beta\Big]. \tag{A12}$$

We use the following parameters:

$$\mu = \frac{m_\pi}{M_{sc}} \quad R = \frac{M_\Delta}{M_N} \quad r = \frac{M_N}{M_\Delta} \quad \tilde{q}^2 = \frac{q^2}{M_N^2} \tag{A13}$$

$$C_{NN} = \frac{g_A M_{sc}}{8 f_\pi \pi} \quad C_{ND} = \frac{h_A M_{sc}}{8 f_\pi \pi} \quad C_{DD} = \frac{H_A M_{sc}}{8 f_\pi \pi}. \tag{A14}$$

APPENDIX B: NUCLEON ELECTROMAGNETIC FORM FACTORS

For the nucleon electromagnetic form factors we take the mass scale $M_{sc} = M_N$ and the following functions occur:

$$\tilde{\mathcal{M}}_1 = z\mu^2 + (1-z)^2 - z^2x(1-x)\tilde{q}^2,$$
$$\tilde{\mathcal{M}}_2 = (1-z)\mu^2 + z^2 - z^2x(1-x)\tilde{q}^2,$$
$$\tilde{\mathcal{M}}_3 = z\mu^2 - z(1-z) + (1-z)R^2 - z^2x(1-x)\tilde{q}^2,$$
$$\tilde{\mathcal{M}}_4 = (1-z)\mu^2 - z(1-z) + zR^2 - z^2x(1-x)\tilde{q}^2,$$
$$\tilde{\mathcal{M}}_{78} = z\mu^2 - z(1-z) + (1-z)R^2, \tag{B1}$$

with $\tilde{q}^2 = q^2/M_N^2$. The isospin factors are:

$$I_{N1} = \begin{pmatrix} +2 \\ -2 \end{pmatrix} \quad I_{N2} = \begin{pmatrix} +1 \\ +2 \end{pmatrix} \quad I_{N3} = \begin{pmatrix} -\frac{2}{3} \\ +\frac{2}{3} \end{pmatrix}$$
$$I_{N4} = \begin{pmatrix} +\frac{8}{3} \\ -\frac{2}{3} \end{pmatrix} \quad I_{N78a} = \begin{pmatrix} -\frac{2}{3} \\ +\frac{2}{3} \end{pmatrix}$$
$$I_{N78b} = \begin{pmatrix} +\frac{8}{3} \\ -\frac{2}{3} \end{pmatrix} \quad I_{NT1} = \begin{pmatrix} +1 \\ -1 \end{pmatrix}. \tag{B2}$$

In case of the unintegrated versions the densities have to be integrated by:

$$F(q^2) = \int_0^1 dz \int_0^1 dx \mathcal{F}(q^2, z, x) \tag{B3}$$

with

$$\mathcal{L}_i = \ln[\tilde{\mathcal{M}}_i].$$

The integrated isovector versions contain the following expression:

$$\mathcal{A} = \frac{1}{\Gamma}\left(\arctan\frac{1 + R^2 - \mu^2}{\Gamma} + \arctan\frac{1 - R^2 + \mu^2}{\Gamma}\right)$$
$$\Gamma = \sqrt{-R^4 - (-1+\mu^2)^2 + 2R^2(1+\mu^2)}. \tag{B4}$$

In the following expressions for the nucleon quantities we renormalized already the infinite terms proportional to L. However, the power-counting breaking terms (constant in m_π terms) are still kept at this stage. Furthermore, we use the notation $dF_i = \frac{d}{dq^2}|_{q^2=0}F_i(q^2)$ and list only contributions to the derivatives of $F_1(q^2)$ and $F_2(q^2)$ or to the nucleon anomalous magnetic moment.

1. Contributions to $F_1(q^2)$

Contributions from virtual nucleons:

$$\frac{\mathcal{F}_1^{N1}}{C_{NN}^2 I_{N1}} = -6z + 14z^2 - 12xz^2 - 4z^3 + 4xz^3 + (-15z - 3\tilde{\mathcal{M}}_1 z + 42z^2 - 36xz^2 - 17z^3 + 16xz^3)\mathcal{L}_1 + 2\tilde{\mathcal{M}}_1 z + (-2z + 10z^2 - 4xz^2 - 18z^3 + 12xz^3 + 14z^4 - 12xz^4 - 4z^5 + 4xz^5)[1/\tilde{\mathcal{M}}_1] + \tilde{q}^2(xz^3 - x^2z^3)\mathcal{L}_1 + \tilde{q}^2(6xz^3 - 6x^2z^3 - 14xz^4 + 26x^2z^4 - 12x^3z^4 + 4xz^5 - 8x^2z^5 + 4x^3z^5)[1/\tilde{\mathcal{M}}_1] \tag{B5}$$

$$\frac{\mathcal{F}_1^{N2}}{C_{NN}^2 I_{N2}} = -4z - \tilde{\mathcal{M}}_2 z + 4z^2 - 8xz^2 + 2z^3 + \mathcal{L}_2(-6z + 6\tilde{\mathcal{M}}_2 z + 12z^2 - 24xz^2 + 6z^3) + [1/\tilde{\mathcal{M}}_2](4z^4 - 8xz^4 + z^5) + \tilde{q}^4[1/\tilde{\mathcal{M}}_2](xz^3 - x^2z^3 - xz^4 + x^2z^4 + x^2z^5 - 2x^3z^5 + x^4z^5) + \tilde{q}^2(z^2 - 2xz^3 + 2x^2z^3 + \mathcal{L}_2(-z + 3z^2 - 6xz^3 + 6x^2z^3) + [1/\tilde{\mathcal{M}}_2](4xz^3 - 4x^2z^3 + z^4 - 4xz^4 + 12x^2z^4 - 8x^3z^4 - 2xz^5 + 2x^2z^5)) \tag{B6}$$

$$\mathcal{F}_1^{NT1} = \frac{I_{NT1} M_N^2}{32 f_\pi^2 \pi^2}(\tilde{q}^2(-1+x)x + \mu^2)(-1 + \ln[\tilde{q}^2(-1+x)x + \mu^2]) \tag{B7}$$

Contributions from virtual $\Delta(1232)$ with minimal $\gamma\Delta\Delta$ coupling:

$$\frac{18R^2\mathcal{F}_1^{N3}}{C_{ND}^2 I_{N3}} = -36Rz - 36z^2 + 80Rz^2 - 88Rxz^2 + 80z^3 - 88xz^3 + \mathcal{L}_3(18\tilde{\mathcal{M}}_3 z - 36Rz - 36z^2 + 96Rz^2 - 120Rxz^2 + 96z^3 - 120xz^3) + \tilde{q}^2(16\tilde{\mathcal{M}}_3 z + 20Rz + 20z^2 - 42Rz^2 + 44Rxz^2 - 42z^3 + 40xz^3 + 4x^2z^3 + \mathcal{L}_3(-24\tilde{\mathcal{M}}_3 z + 24Rz + 24z^2 - 63Rz^2 + 60Rxz^2 - 63z^3 + 48xz^3 + 12x^2z^3) + [1/\tilde{\mathcal{M}}_3](24Rxz^3 - 24Rx^2z^3 + 24xz^4 - 48Rxz^4 - 24x^2z^4 + 96Rx^2z^4 - 48Rx^3z^4 - 48xz^5 + 96x^2z^5 - 48x^3z^5)) + \tilde{q}^4(-xz^3 + x^2z^3 + \mathcal{L}_3(6xz^3 - 6x^2z^3) + [1/\tilde{\mathcal{M}}_3](-6Rxz^3 + 6Rx^2z^3 - 6xz^4 + 12Rxz^4 + 6x^2z^4 - 24Rx^2z^4 + 12Rx^3z^4 + 12xz^5 - 24x^2z^5 + 12x^3z^5)) \tag{B8}$$

$$\frac{54R^4\mathcal{F}_1^{N4}}{C_{ND}^2 I_{N4}} = -54R^2z + 54\tilde{\mathcal{M}}_4 R^2 z - 108R^3z - 54R^4z + 240R^2z^2 + 240R^3z^2 - 264R^2xz^2 - 264R^3xz^2 - 186R^2z^3 + 264R^2xz^3 + \mathcal{L}_4(-54R^2z + 108\tilde{\mathcal{M}}_4R^2z - 108R^3z - 54R^4z + 288R^2z^2 + 288R^3z^2 - 360R^2xz^2 - 360R^3xz^2 - 234R^2z^3 + 360R^2xz^3) + \tilde{q}^2(-8z + 30Rz + 48R^2z - 26R^3z - 36R^4z - 16z^2 - 79Rz^2 - 138R^2z^2 - 75R^3z^2 - 48Rxz^2 + 36R^2xz^2 + 84R^3xz^2 + 56z^3 + 100Rz^3 + 162R^2z^3 - 258R^2xz^3 + 126R^2x^2z^3 - 32z^4 - 51Rz^4 + 48Rxz^4 + \tilde{\mathcal{M}}_4(30z + 86Rz + 60R^2z - 38z^2 - 69Rz^2 + 84Rxz^2) + [1/\tilde{\mathcal{M}}_4](36R^2xz^3 + 72R^3xz^3 + 36R^4xz^3 - 36R^2x^2z^3 - 72R^3x^2z^3 - 36R^4x^2z^3 - 144R^2xz^4 - 144R^3xz^4 + 288R^2x^2z^4 + 288R^3x^2z^4 - 144R^2x^3z^4 - 144R^3x^3z^4 + 108R^2xz^5 - 252R^2x^2z^5 + 144R^2x^3z^5) + \mathcal{L}_4(6z + 18Rz + 18R^2z + 6R^3z - 42z^2 - 33Rz^2 - 135R^2z^2 - 144R^3z^2 - 36Rxz^2 + 108R^2xz^2 + 144R^3xz^2 + 66z^3 + 60Rz^3 + 189R^2z^3 - 342R^2xz^3 + 162R^2x^2z^3 - 30z^4 - 45Rz^4 + 36Rxz^4 + \tilde{\mathcal{M}}_4(108z + 120Rz + 72R^2z - 120z^2 - 180Rz^2 + 144Rxz^2))) \tag{B9}$$

$$\frac{R^2\mathcal{F}_1^{N78}}{2C_{ND}^2} = (I_{N78a} + I_{N78b})\mathcal{M}_{78}(R+z)\ln\tilde{\mathcal{M}}_{78} \tag{B10}$$

Additional contribution from nonminimal $\gamma\Delta\Delta$ coupling:

$$\frac{27R^5\mathcal{F}_1^{nm}}{C_{ND}^2 I_{N4}} = \tilde{q}^2(-24z - 20Rz + 24R^2z + 12R^3z - 8R^4z + 72z^2 + 116Rz^2 + 41R^2z^2 - 3R^3z^2 - 72z^3 - 172Rz^3 - 65R^2z^3 + 24z^4 + 76Rz^4 + \tilde{\mathcal{M}}_4(-42z - 198Rz - 115R^2z + 42z^2 + 178Rz^2) + \mathcal{L}_4(-18z - 12Rz + 27R^2z + 18R^3z - 3R^4z + 54z^2 + 66Rz^2 - 15R^2z^2 - 27R^3z^2 - 54z^3 - 96Rz^3 - 12R^2z^3 + 18z^4 + 42Rz^4 + \tilde{\mathcal{M}}_4(-72z - 198Rz - 96R^2z + 72z^2 + 168Rz^2))) \tag{B11}$$

2. Contributions to $F_2(q^2)$

Contributions from virtual nucleons:

$$\frac{\mathcal{F}_2^{N1}}{C_{NN}^2 I_{N1}} = 6z - 14z^2 + 12xz^2 + 4z^3 - 4xz^3 + (12z - 42z^2 + 36xz^2 + 16z^3 - 16xz^3)\mathcal{L}_1 + (2z - 10z^2 + 4xz^2 + 18z^3 - 12xz^3 - 14z^4 + 12xz^4 + 4z^5 - 4xz^5)[1/\tilde{\mathcal{M}}_1] + \tilde{q}^2(-6xz^3 + 6x^2z^3 + 14xz^4 - 26x^2z^4 + 12x^3z^4 - 4xz^5 + 8x^2z^5 - 4x^3z^5)[1/\tilde{\mathcal{M}}_1] \quad \text{(B12)}$$

$$\frac{\mathcal{F}_2^{N2}}{C_{NN}^2 I_{N2}} = -8z^2 + 8xz^2 + \mathcal{L}_2(8z - 24z^2 + 24xz^2) + [1/\tilde{\mathcal{M}}_2](-8z^4 + 8xz^4) + \tilde{q}^2[1/\tilde{\mathcal{M}}_2](-8xz^3 + 8x^2z^3 + 8xz^4 - 16x^2z^4 + 8x^3z^4) \quad \text{(B13)}$$

Contributions from virtual Δ(1232) with minimal $\gamma\Delta\Delta$ coupling:

$$\frac{9R^2\mathcal{F}_2^{N3}}{C_{ND}^2 I_{N3}} = -28\tilde{\mathcal{M}}_3 z + 18Rz + 18z^2 - 44Rz^2 + 44Rxz^2 - 44z^3 + 44xz^3 + \mathcal{L}_3(24\tilde{\mathcal{M}}_3 z + 18Rz + 18z^2 - 42Rz^2 + 60Rxz^2 - 42z^3 + 60xz^3) + [1/\tilde{\mathcal{M}}_3]\tilde{q}^4(3Rxz^3 - 3Rx^2z^3 + 3xz^4 - 6Rxz^4 - 3x^2z^4 + 12Rx^2z^4 - 6Rx^3z^4 - 6xz^5 + 12x^2z^5 - 6x^3z^5) + \tilde{q}^2(-10Rz - 10z^2 + 22Rz^2 - 22Rxz^2 + 22z^3 - 18xz^3 - 4x^2z^3 + \mathcal{L}_3(-12Rz - 12z^2 + 30Rz^2 - 30Rxz^2 + 30z^3 - 36xz^3 + 6x^2z^3) + [1/\tilde{\mathcal{M}}_3](-12Rxz^3 + 12Rx^2z^3 - 12xz^4 + 24Rxz^4 + 12x^2z^4 - 48Rx^2z^4 + 24Rx^3z^4 + 24xz^5 - 48x^2z^5 + 24x^3z^5)) \quad \text{(B14)}$$

$$\frac{27R^4\mathcal{F}_2^{N4}}{2C_{ND}^2 I_{N4}} = 8z - 30Rz - 42R^2z + 38R^3z + 42R^4z - 24z^2 + 63Rz^2 + 18R^2z^2 - 69R^3z^2 + 66R^2xz^2 + 66R^3xz^2 + 24z^3 - 36Rz^3 + 24R^2z^3 - 66R^2xz^3 - 8z^4 + 3Rz^4 + \tilde{\mathcal{M}}_4(50z - 4Rz - 48R^2z - 50z^2 - 15Rz^2) + \mathcal{L}_4(-6z - 18Rz + 30R^3z + 18R^4z + 18z^2 + 45Rz^2 - 45R^2z^2 - 72R^3z^2 + 90R^2xz^2 + 90R^3xz^2 - 18z^3 - 36Rz^3 + 45R^2z^3 - 90R^2xz^3 + 6z^4 + 9Rz^4 + \tilde{\mathcal{M}}_4(-24z - 78Rz - 90R^2z + 24z^2 + 36Rz^2)) + \tilde{q}^2(2z + 2Rz - 2R^2z - 2R^3z - 6z^2 - 39Rz^2 - 12R^2z^2 + 21R^3z^2 + 12Rxz^2 - 9R^2xz^2 - 21R^3xz^2 - 2z^3 + 17Rz^3 - 33R^2z^3 + 44xz^3 + 24Rxz^3 + 126R^2xz^3 - 44x^2z^3 - 24Rx^2z^3 - 93R^2x^2z^3 + 6z^4 + 12Rz^4 - 44xz^4 - 15Rxz^4 + 44x^2z^4 + 3Rx^2z^4 + \tilde{\mathcal{M}}_4(-9z - 5Rz + 24z^2 + 21Rz^2 - 21Rxz^2) + [1/\tilde{\mathcal{M}}_4](12xz^3 + 18Rxz^3 - 9R^2xz^3 - 24R^3xz^3 - 9R^4xz^3 - 12x^2z^3 - 18Rx^2z^3 + 9R^2x^2z^3 + 24R^3x^2z^3 + 9R^4x^2z^3 - 36xz^4 - 36Rxz^4 + 36R^2xz^4 + 36R^3xz^4 + 36x^2z^4 + 36Rx^2z^4 - 72R^2x^2z^4 - 72R^3x^2z^4 + 36R^2x^3z^4 + 36R^3x^3z^4 + 36xz^5 + 18Rxz^5 - 27R^2xz^5 - 36x^2z^5 - 18Rx^2z^5 + 63R^2x^2z^5 - 36R^2x^3z^5 - 12xz^6 + 12x^2z^6) + \mathcal{L}_4(3z + 3Rz - 3R^2z - 3R^3z - 18z^2 - 36Rz^2 + 18R^2z^2 + 36R^3z^2 + 9Rxz^2 - 27R^2xz^2 - 36R^3xz^2 + 15z^3 + 12Rz^3 - 45R^2z^3 + 66xz^3 + 54Rxz^3 + 108R^2xz^3 - 66x^2z^3 - 54Rx^2z^3 - 63R^2x^2z^3 + 9Rz^4 - 66xz^4 - 18Rxz^4 + 66x^2z^4 + 9Rx^2z^4 + \tilde{\mathcal{M}}_4(6Rz + 36Rz^2 - 36Rxz^2))) \quad \text{(B15)}$$

$$\frac{9R^3\mathcal{F}_2^{N78}}{4C_{ND}^2} = -\tilde{\mathcal{M}}_{78}(R + z)(-I_{N78b} - I_{N78a}R - I_{N78b}R + (6I_{N78a}R + I_{N78b}(-3 + 6R))\ln\mathcal{M}_{78}) \quad \text{(B16)}$$

Additional contribution from nonminimal $\gamma\Delta\Delta$ vertex:

$$\frac{27R^5\mathcal{F}_2^{nm}}{C_{ND}^2 I_{N4}} = 80Rz + 126R^2z + 12R^3z - 34R^4z - 240Rz^2 - 252R^2z^2 - 12R^3z^2 + 240Rz^3 + 126R^2z^3 - 80Rz^4$$
$$+ \tilde{\mathcal{M}}_4(176Rz + 170R^2z - 176Rz^2) + \mathcal{L}_4(48Rz + 18R^2z - 108R^3z - 78R^4z - 144Rz^2 - 36R^2z^2$$
$$+ 108R^3z^2 + 144Rz^3 + 18R^2z^3 - 48Rz^4 + \tilde{\mathcal{M}}_4(192Rz + 174R^2z - 192Rz^2)) + \tilde{q}^2(24z - 20Rz - 72R^2z$$
$$+ 12R^3z + 40R^4z - 80z^2 + 90Rz^2 + 164R^2z^2 - 6R^3z^2 + 88z^3 - 52Rz^3 - 16R^2z^3 - 304Rxz^3 - 234R^2xz^3$$
$$+ 304Rx^2z^3 + 234R^2x^2z^3 - 32z^4 - 18Rz^4 + 304Rxz^4 - 304Rx^2z^4 + \tilde{\mathcal{M}}_4(40z + 84Rz + 28R^2z - 38z^2 - 18Rz^2)$$
$$+ [1/\tilde{\mathcal{M}}_4](-24Rxz^3 + 72R^3xz^3 + 48R^4xz^3 + 24Rx^2z^3 - 72R^3x^2z^3 - 48R^4x^2z^3 + 72Rxz^4 - 72R^3xz^4$$
$$- 72Rx^2z^4 + 72R^3x^2z^4 - 72Rxz^5 + 72Rx^2z^5 + 24Rxz^6 - 24Rx^2z^6) + \mathcal{L}_4(18z - 12Rz - 36R^2z + 36R^3z$$
$$+ 42R^4z - 66z^2 + 54Rz^2 + 48R^2z^2 - 72R^3z^2 + 78z^3 - 24Rz^3 + 48R^2z^3 - 168Rxz^3 - 234R^2xz^3 + 168Rx^2z^3$$
$$+ 234R^2x^2z^3 - 30z^4 - 18Rz^4 + 168Rxz^4 - 168Rx^2z^4 + \tilde{\mathcal{M}}_4(114z + 108Rz + 24R^2z - 120z^2 - 72Rz^2))) \tag{B17}$$

3. Isovector Dirac radius $\langle r_1^2\rangle_V$

Contributions from virtual nucleons:

$$dF_1^N = -\frac{\ln\mu}{48f_\pi^2\pi^2} - \frac{C_{NN}^2}{3M_N^2(-4+\mu^2)}\Big(-172 + 163\mu^2 - 30\mu^4 + (-80 + 372\mu^2 - 208\mu^4 + 30\mu^6)\ln\mu$$
$$+ \mu\sqrt{-4+\mu^2}(70 - 74\mu^2 + 15\mu^4)\ln\frac{\mu - \sqrt{-4+\mu^2}}{\mu + \sqrt{-4+\mu^2}}\Big) \tag{B18}$$

Contributions from virtual $\Delta(1232)$ with minimal $\gamma\Delta\Delta$ coupling:

$$\frac{324R^4M_N^2dF_1^\Delta}{C_{ND}^2} = 60 - 20R + 143R^2 + 314R^3 - 611R^4 + 26R^5 + 441R^6 - 44R^7 - 90R^8 - 130\mu^2 - 80R\mu^2$$
$$- 562R^2\mu^2 - 438R^3\mu^2 - 778R^4\mu^2 + 168R^5\mu^2 + 270R^6\mu^2 - 55\mu^4 - 20R\mu^4 + 287R^2\mu^4$$
$$- 204R^3\mu^4 - 270R^4\mu^4 + 50\mu^6 + 80R\mu^6 + 90R^2\mu^6 + \mathcal{A}(70 + 60R + 32R^2 + 124R^3 - 678R^4$$
$$- 664R^5 + 1136R^6 + 432R^7 - 1046R^8 + 92R^9 + 576R^{10} - 44R^{11} - 90R^{12} - 230\mu^2 - 280R\mu^2$$
$$- 418R^2\mu^2 - 108R^3\mu^2 + 424R^4\mu^2 - 8R^5\mu^2 + 888R^6\mu^2 - 676R^7\mu^2 - 1930R^8\mu^2 + 256R^9\mu^2$$
$$+ 450R^{10}\mu^2 + 220\mu^4 + 400R\mu^4 + 972R^2\mu^4 + 560R^3\mu^4 + 1016R^4\mu^4 + 936R^5\mu^4 + 2284R^6\mu^4$$
$$- 584R^7\mu^4 - 900R^8\mu^4 + 20\mu^6 - 120R\mu^6 - 728R^2\mu^6 - 212R^3\mu^6 - 1032R^4\mu^6 + 656R^5\mu^6$$
$$+ 900R^6\mu^6 - 130\mu^8 - 140R\mu^8 + 52R^2\mu^8 - 364R^3\mu^8 - 450R^4\mu^8 + 50\mu^{10} + 80R\mu^{10} + 90R^2\mu^{10})$$
$$+ (-70 - 60R - 102R^2 - 184R^3 + 576R^4 - 480R^5 + 560R^6 - 48R^7 - 486R^8 + 44R^9 + 90R^{10}$$
$$+ 160\mu^2 + 220R\mu^2 + 336R^2\mu^2 + 24R^3\mu^2 + 144R^4\mu^2 + 504R^5\mu^2 + 1264R^6\mu^2 - 212R^7\mu^2$$
$$- 360R^8\mu^2 - 60\mu^4 - 180R\mu^4 - 516R^2\mu^4 - 396R^3\mu^4 - 1020R^4\mu^4 + 372R^5\mu^4 + 540R^6\mu^4 - 80\mu^6$$
$$- 60R\mu^6 + 192R^2\mu^6 - 284R^3\mu^6 - 360R^4\mu^6 + 50\mu^8 + 80R\mu^8 + 90R^2\mu^8)\ln R + (-70 - 60R$$
$$- 102R^2 - 184R^3 + 576R^4 + 480R^5 - 560R^6 + 48R^7 + 486R^8 - 44R^9 - 90R^{10} + 160\mu^2$$
$$+ 220R\mu^2 + 528R^2\mu^2 - 24R^3\mu^2 - 144R^4\mu^2 - 504R^5\mu^2 - 1264R^6\mu^2 + 212R^7\mu^2 + 360R^8\mu^2$$
$$+ 60\mu^4 + 180R\mu^4 + 516R^2\mu^4 + 396R^3\mu^4 + 1020R^4\mu^4 - 372R^5\mu^4 - 540R^6\mu^4 + 80\mu^6$$
$$+ 60R\mu^6 - 192R^2\mu^6 + 284R^3\mu^6 + 360R^4\mu^6 - 50\mu^8 - 80R\mu^8 - 90R^2\mu^8)\ln\mu \tag{B19}$$

Additional contribution from the nonminimal $\gamma\Delta\Delta$ coupling:

$$\frac{162R^5M_N^2dF_1^\Delta}{C_{ND}^2} = -40 - 100R + 260R^3 + 45R^4 - 185R^5 - 430R^6 + 30R^7 + 100R^8 + 130\mu^2 + 70R\mu^2 - 30R^2\mu^2 + 230R^3\mu^2 + 240R^4\mu^2 - 190R^5\mu^2 - 300R^6\mu^2 - 105\mu^4 + 155R\mu^4 + 160R^2\mu^4 + 290R^3\mu^4 + 300R^4\mu^4 + 30\mu^6 - 130R\mu^6 - 100R^2\mu^6 + \mathcal{A}(-30 - 170R - 120R^2 + 650R^3 + 820R^4 - 960R^5 - 1540R^6 + 680R^7 + 1350R^8 - 230R^9 - 580R^{10} + 30R^{11} + 100R^{12} + 150\mu^2 + 550R\mu^2 + 410R^2\mu^2 - 520R^3\mu^2 - 630R^4\mu^2 - 620R^5\mu^2 - 830R^6\mu^2 + 840R^7\mu^2 + 1400R^8\mu^2 - 250R^9\mu^2 - 500R^{10}\mu^2 - 300\mu^4 - 500R\mu^4 - 410R^2\mu^4 - 360R^3\mu^4 - 340R^4\mu^4 - 640R^5\mu^4 - 750R^6\mu^4 + 700R^7\mu^4 + 1000R^8\mu^4 + 300\mu^6 - 100R\mu^6 - 30R^2\mu^6 - 320R^3\mu^6 - 350R^4\mu^6 - 900R^5\mu^6 - 1000R^6\mu^6 - 150\mu^8 + 350R\mu^8 + 250R^2\mu^8 + 550R^3\mu^8 + 500R^4\mu^8 + 30\mu^{10} - 130R\mu^{10} - 100R^2\mu^{10}) + (30 + 170R + 150R^2 - 480R^3 - 670R^4 - 480R^5 - 870R^6 + 200R^7 + 480R^8 - 30R^9 - 100R^{10} - 120\mu^2 - 380R\mu^2 - 320R^2\mu^2 - 480R^5\mu^2 - 720R^6\mu^2 + 220R^7\mu^2 + 400R^8\mu^2 + 180\mu^4 + 120R\mu^4 + 90R^2\mu^4 + 60R^3\mu^4 + 30R^4\mu^4 - 480R^5\mu^4 - 600R^6\mu^4 - 120\mu^6 + 220R\mu^6 + 180R^2\mu^6 + 420R^3\mu^6 + 400R^4\mu^6 + 30\mu^8 - 130R\mu^8 - 100R^2\mu^8)\ln R + (30 + 170R + 150R^2 - 480R^3 - 670R^4 + 480R^5 + 870R^6 - 200R^7 - 480R^8 + 30R^9 + 100R^{10} - 120\mu^2 - 380R\mu^2 - 320R^2\mu^2 + 480R^5\mu^2 + 720R^6\mu^2 - 220R^7\mu^2 - 400R^8\mu^2 - 180\mu^4 - 120R\mu^4 - 90R^2\mu^4 - 60R^3\mu^4 - 30R^4\mu^4 + 480R^5\mu^4 + 600R^6\mu^4 + 120\mu^6 - 220R\mu^6 - 180R^2\mu^6 - 420R^3\mu^6 - 400R^4\mu^6 - 30\mu^8 + 130R\mu^8 + 100R^2\mu^8)\ln\mu \quad \text{(B20)}$$

4. Isovector anomalous magnetic moment κ_V

Contributions from virtual nucleons:

$$\frac{F_2^N}{4C_{NN}^2} = \frac{1}{\sqrt{-4+\mu^2}}\left((5-6\mu^2)\sqrt{-4+\mu^2} + 2\mu^2\sqrt{-4+\mu^2}(-7+3\mu^2)\ln\mu + \mu(8-13\mu^2+3\mu^4)\ln\frac{\mu-\sqrt{-4+\mu^2}}{\mu+\sqrt{-4+\mu^2}}\right) \quad \text{(B21)}$$

Contributions from virtual Δ(1232) with minimal $\gamma\Delta\Delta$ coupling:

$$\frac{81R^4F_2^\Delta}{C_{N\Delta}^2} = -40 - 100R - 153R^2 + 220R^3 + 697R^4 + 88R^5 - 191R^6 + 40R^7 + 54R^8 + 150\mu^2 + 140R\mu^2 + 522R^2\mu^2 + 356R^3\mu^2 + 230R^4\mu^2 - 120R^5\mu^2 - 162R^6\mu^2 - 35\mu^4 + 60R\mu^4 - 49R^2\mu^4 + 120R^3\mu^4 + 162R^4\mu^4 + 10\mu^6 - 40R\mu^6 - 54R^2\mu^6 + \mathcal{A}(-10 - 40R - 64R^2 + 188R^3 + 434R^4 - 292R^5 - 800R^6 + 220R^7 + 658R^8 - 116R^9 - 272R^{10} + 40R^{11} + 54R^{12} + 50\mu^2 + 120R\mu^2 + 342R^2\mu^2 - 4R^3\mu^2 - 552R^4\mu^2 - 648R^5\mu^2 - 632R^6\mu^2 + 444R^7\mu^2 + 774R^8\mu^2 - 200R^9\mu^2 - 270R^{10}\mu^2 - 100\mu^4 - 80R\mu^4 - 588R^2\mu^4 - 356R^3\mu^4 - 328R^4\mu^4 - 420R^5\mu^4 - 700R^6\mu^4 + 400R^7\mu^4 + 540R^8\mu^4 + 100\mu^6 - 80R\mu^6 + 352R^2\mu^6 - 28R^3\mu^6 + 176R^4\mu^6 - 400R^5\mu^6 - 540R^6\mu^6 - 50\mu^8 + 120R\mu^8 + 12R^2\mu^8 + 200R^3\mu^8 + 270R^4\mu^8 + 10\mu^{10} - 40R\mu^{10} - 54R^2\mu^{10}) + (10 + 40R + 74R^2 - 148R^3 - 360R^4 - 576R^5 - 440R^6 + 76R^7 + 218R^8 - 40R^9 - 54R^{10} - 40\mu^2 - 80R\mu^2 - 288R^2\mu^2 - 144R^3\mu^2 + 72R^4\mu^2 - 288R^5\mu^2 - 448R^6\mu^2 + 160R^7\mu^2 + 216R^8\mu^2 + 60\mu^4 + 300R^2\mu^4 + 132R^3\mu^4 + 252R^4\mu^4 - 240R^5\mu^4 - 324R^6\mu^4 - 40\mu^6 + 80R\mu^6 - 32R^2\mu^6 + 160R^3\mu^6 + 216R^4\mu^6 + 10\mu^8 - 40R\mu^8 - 54R^2\mu^8)\ln R + (10 + 40R + 74R^2 - 148R^3 - 360R^4 + 144R^5 + 440R^6 - 76R^7 - 218R^8 + 40R^9 + 54R^{10} - 40\mu^2 - 80R\mu^2 - 432R^2\mu^2 - 288R^3\mu^2 - 72R^4\mu^2 + 288R^5\mu^2 + 448R^6\mu^2 - 160R^7\mu^2 - 216R^8\mu^2 - 60\mu^4 - 300R^2\mu^4 - 132R^3\mu^4 - 252R^4\mu^4 + 240R^5\mu^4 + 324R^6\mu^4 + 40\mu^6 - 80R\mu^6 + 32R^2\mu^6 - 160R^3\mu^6 - 216R^4\mu^6 - 10\mu^8 + 40R\mu^8 + 54R^2\mu^8)\ln\mu \quad \text{(B22)}$$

Additional contribution from the nonminimal $\gamma\Delta\Delta$ coupling:

$$\frac{81R^4F_2^\Delta}{C_{N\Delta}^2} = 40 + 180R + 280R^2 + 340R^3 + 140R^4 + 80R^5 - 160R^6 - 100R^7 - 120\mu^2 - 100R\mu^2 + 120R^2\mu^2$$
$$+ 40R^3\mu^2 + 280R^4\mu^2 + 300R^5\mu^2 + 140\mu^4 - 120R\mu^4 - 80R^2\mu^4 - 300R^3\mu^4 - 40\mu^6 + 100R\mu^6$$
$$+ \mathcal{A}(40 + 130R - 20R^2 - 320R^3 - 20R^4 + 280R^5 - 220R^6 - 220R^7 + 380R^8 + 230R^9 - 160R^{10}$$
$$- 100R^{11} - 200\mu^2 - 420R\mu^2 + 60R^2\mu^2 + 220R^3\mu^2 - 120R^4\mu^2 + 120R^5\mu^2 - 340R^6\mu^2 - 420R^7\mu^2$$
$$+ 600R^8\mu^2 + 500R^9\mu^2 + 400\mu^4 + 380R\mu^4 - 60R^2\mu^4 + 20R^3\mu^4 - 260R^4\mu^4 - 120R^5\mu^4 - 800R^6\mu^4$$
$$- 1000R^7\mu^4 - 400\mu^6 + 80R\mu^6 + 20R^2\mu^6 + 580R^3\mu^6 + 400R^4\mu^6 + 1000R^5\mu^6 + 200\mu^8$$
$$- 270R\mu^8 - 500R^3\mu^8 - 40\mu^{10} + 100R\mu^{10}) + (-40 - 130R - 20R^2 + 190R^3 + 90R^5 - 220R^6 - 130R^7$$
$$+ 160R^8 + 100R^9 + 160\mu^2 + 290R\mu^2 + 90R^5\mu^2 - 440R^6\mu^2 - 400R^7\mu^2 - 240\mu^4 - 90R\mu^4$$
$$+ 60R^2\mu^4 + 210R^3\mu^4 + 360R^4\mu^4 + 600R^5\mu^4 + 160\mu^6 - 170R\mu^6 - 40R^2\mu^6 - 400R^3\mu^6$$
$$- 40\mu^8 + 100R\mu^8)\ln R + (-40 - 130R - 20R^2 + 190R^3 - 90R^5 + 220R^6 + 130R^7 - 160R^8 - 100R^9$$
$$+ 160\mu^2 + 290R\mu^2 - 90R^5\mu^2 + 440R^6\mu^2 + 400R^7\mu^2 + 240\mu^4 + 90R\mu^4 - 60R^2\mu^4 - 210R^3\mu^4$$
$$- 360R^4\mu^4 - 600R^5\mu^4 - 160\mu^6 + 170R\mu^6 + 40R^2\mu^6 + 400R^3\mu^6 + 40\mu^8 - 100R\mu^8)\ln\mu \tag{B23}$$

5. Isovector Pauli radius $\langle r_2^2\rangle_V$

Contributions from virtual nucleons:

$$dF_2^N = \frac{2C_{NN}^2}{3M_N^2\mu(-4+\mu^2)^{3/2}}\Big(\mu\sqrt{-4+\mu^2}(-124 + 105\mu^2 - 18\mu^4) + 6\mu\sqrt{-4+\mu^2}(-16 + 44\mu^2 - 22\mu^4 + 3\mu^6)\ln\mu$$
$$+ (16 - 216\mu^2 + 246\mu^4 - 84\mu^6 + 9\mu^8)\ln\frac{\mu - \sqrt{-4+\mu^2}}{\mu + \sqrt{-4+\mu^2}}\Big) \tag{B24}$$

Contributions from virtual $\Delta(1232)$ with minimal $\gamma\Delta\Delta$ coupling:

$$\frac{486R^4M_N^2dF_2^\Delta}{C_{ND}^2} = -90 + 280R - 171R^2 - 1106R^3 + 108R^4 + 186R^5 - 675R^6 + 132R^7 + 162R^8 - 340R\mu^2$$
$$+ 198R^2\mu^2 + 162R^3\mu^2 + 1116R^4\mu^2 - 504R^5\mu^2 - 486R^6\mu^2 + 270\mu^4 + 300R\mu^4 - 261R^2\mu^4$$
$$+ 612R^3\mu^4 + 486R^4\mu^4 - 180\mu^6 - 240R\mu^6 - 162R^2\mu^6 + \mathcal{A}(300R - 126R^2 - 1500R^3 + 378R^4$$
$$+ 2712R^5 - 540R^6 - 1488R^7 + 1188R^8 - 12R^9 - 918R^{10} + 132R^{11} + 162R^{12} - 600R\mu^2 + 342R^2\mu^2$$
$$+ 948R^3\mu^2 + 576R^4\mu^2 + 576R^5\mu^2 - 1044R^6\mu^2 + 348R^7\mu^2 + 2952R^8\mu^2 - 768R^9\mu^2 - 810R^{10}\mu^2$$
$$+ 180\mu^4 + 480R\mu^4 - 648R^2\mu^4 + 216R^3\mu^4 - 936R^4\mu^4 - 3168R^6\mu^4 + 1752R^7\mu^4 + 1620R^8\mu^4$$
$$- 540\mu^6 - 600R\mu^6 + 252R^2\mu^6 - 996R^3\mu^6 + 972R^4\mu^6 - 1968R^5\mu^6 - 1620R^6\mu^6 + 540\mu^8 + 660R\mu^8$$
$$+ 342R^2\mu^8 + 1092R^3\mu^8 + 810R^4\mu^8 - 180\mu^{10} - 240R\mu^{10} - 162R^2\mu^{10}) + (-300R + 126R^2 + 1440R^3$$
$$+ 108R^4 + 1368R^5 - 432R^6 - 120R^7 + 756R^8 - 132R^9 - 162R^{10} + 300R\mu^2 - 216R^2\mu^2 + 192R^3\mu^2$$
$$- 72R^4\mu^2 - 96R^5\mu^2 - 1872R^6\mu^2 + 636R^7\mu^2 + 648R^8\mu^2 - 180\mu^4 - 180R\mu^4 + 252R^2\mu^4 - 204R^3\mu^4$$
$$+ 1296R^4\mu^4 - 1116R^5\mu^4 - 972R^6\mu^4 + 360\mu^6 + 420R\mu^6 + 852R^3\mu^6 + 648R^4\mu^6 - 180\mu^8$$
$$- 240R\mu^8 - 162R^2\mu^8)\ln R + (-300R + 270R^2 + 1344R^3 - 108R^4 - 1368R^5 + 432R^6 + 120R^7$$
$$- 756R^8 + 132R^9 + 162R^{10} + 300R\mu^2 + 216R^2\mu^2 - 192R^3\mu^2 + 72R^4\mu^2 + 96R^5\mu^2 + 1872R^6\mu^2$$
$$- 636R^7\mu^2 - 648R^8\mu^2 + 180\mu^4 + 180R\mu^4 - 252R^2\mu^4 + 204R^3\mu^4 - 1296R^4\mu^4 + 1116R^5\mu^4 + 972R^6\mu^4$$
$$- 360\mu^6 - 420R\mu^6 - 852R^3\mu^6 - 648R^4\mu^6 + 180\mu^8 + 240R\mu^8 + 162R^2\mu^8)\ln\mu \tag{B25}$$

Additional contribution from the nonminimal $\gamma\Delta\Delta$ coupling:

$$\frac{243R^5M_N^2dF_2^\Delta}{C_{ND}^2} = 120 + 60R + 25R^2 + 390R^3 - 125R^4 + 420R^6 - 120R^8 - 270\mu^2 + 60R\mu^2 + 65R^2\mu^2 - 720R^3\mu^2$$
$$- 270R^4\mu^2 + 360R^5\mu^2 + 360R^6\mu^2 + 90\mu^4 - 540R\mu^4 - 150R^2\mu^4 - 720R^3\mu^4 - 360R^4\mu^4 + 360R\mu^6$$
$$+ 120R^2\mu^6 + \mathcal{A}(90 + 180R - 60R^2 - 540R^3 - 600R^4 + 540R^5 + 1380R^6 - 180R^7 - 1290R^8$$
$$+ 600R^{10} - 120R^{12} - 360\mu^2 - 540R\mu^2 - 60R^2\mu^2 + 360R^3\mu^2 + 750R^4\mu^2 + 1080R^5\mu^2 + 540R^6\mu^2$$
$$- 1260R^7\mu^2 - 1470R^8\mu^2 + 360R^9\mu^2 + 600R^{10}\mu^2 + 540\mu^4 + 180R\mu^4 + 210R^2\mu^4 + 720R^3\mu^4$$
$$+ 540R^4\mu^4 + 1440R^5\mu^4 + 810R^6\mu^4 - 1440R^7\mu^4 - 1200R^8\mu^4 - 360\mu^6 + 900R\mu^6 + 120R^2\mu^6$$
$$+ 900R^3\mu^6 + 390R^4\mu^6 + 2160R^5\mu^6 + 1200R^6\mu^6 + 90\mu^8 - 1080R\mu^8 - 330R^2\mu^8 - 1440R^3\mu^8$$
$$- 600R^4\mu^8 + 360R\mu^{10} + 120R^2\mu^{10}) + (-90 - 180R - 30R^2 + 360R^3 + 1170R^4 + 180R^5 + 810R^6$$
$$- 480R^8 + 120R^{10} + 270\mu^2 + 360R\mu^2 + 120R^2\mu^2 + 300R^4\mu^2 + 900R^5\mu^2 + 750R^6\mu^2 - 360R^7\mu^2$$
$$- 480R^8\mu^2 - 270\mu^4 + 180R\mu^4 - 180R^3\mu^4 - 60R^4\mu^4 + 1080R^5\mu^4 + 720R^6\mu^4 + 90\mu^6 - 720R\mu^6$$
$$- 210R^2\mu^6 - 1080R^3\mu^6 - 480R^4\mu^6 + 360R\mu^8 + 120R^2\mu^8)\ln R + (-90 - 180R - 30R^2 + 360R^3$$
$$+ 570R^4 - 180R^5 - 810R^6 + 480R^8 - 120R^{10} + 270\mu^2 + 360R\mu^2 + 120R^2\mu^2 - 300R^4\mu^2 - 900R^5\mu^2$$
$$- 750R^6\mu^2 + 360R^7\mu^2 + 480R^8\mu^2 + 270\mu^4 - 180R\mu^4 + 180R^3\mu^4 + 60R^4\mu^4 - 1080R^5\mu^4$$
$$- 720R^6\mu^4 - 90\mu^6 + 720R\mu^6 + 210R^2\mu^6 + 1080R^3\mu^6 + 480R^4\mu^6 - 360R\mu^8 - 120R^2\mu^8)\ln\mu \quad \text{(B26)}$$

6. Renormalized constants

The constants are with $\tilde{\delta} = \delta^2R^2(R+1)^2$:

$$c_r \cdot (f_\pi 8\pi)^2 = -\frac{43g_A^2}{3} + \frac{h_A^2}{324R^5}(60R - 20R^2 + 143R^3 + 314R^4 - 611R^5 + 26R^6 + 441R^7 - 44R^8 - 90R^9$$
$$+ (12R^3 + 24R^4 - 96R^5 - 960R^6 + 1120R^7 - 96R^8 - 972R^9 + 88R^{10} + 180R^{11})\ln R$$
$$+ (1+R)^2(-35R + 40R^2 - 96R^3 + 60R^4 + 264R^5 - 348R^6 + 152R^7 + 68R^8 - 45R^9)\ln\tilde{\delta})$$
$$+ \frac{h_A^2\kappa_{nm}}{324R^5}(-80 - 200R + 520R^3 + 90R^4 - 370R^5 - 860R^6 + 60R^7 + 200R^8 + (-1920R^5 - 3480R^6$$
$$+ 800R^7 + 1920R^8 - 120R^9 - 400R^{10})\ln R + (1+R)^2(30 + 110R - 100R^2 - 390R^3 + 210R^4$$
$$+ 450R^5 - 240R^6 - 170R^7 + 100R^8)\ln\tilde{\delta}), \quad \text{(B27)}$$

$$c_\kappa \cdot \frac{(f_\pi 8\pi)^2}{M_N^2} = 20g_A^2 + \frac{h_A^2}{81R^4}(-40 - 100R - 153R^2 + 220R^3 + 697R^4 + 88R^5 - 191R^6 + 40R^7 + 54R^8$$
$$+ (-720R^5 - 880R^6 + 152R^7 + 436R^8 - 80R^9 - 108R^{10})\ln R + \delta R(1+R)^3(-5 - 10R - 17R^2 + 98R^3$$
$$- 41R^4 - 34R^5 + 27R^6)\ln\tilde{\delta}) + \frac{h_A^2\kappa_{nm}}{81R^4}(40 + 180R + 280R^2 + 340R^3 + 140R^4 + 80R^5 - 160R^6$$
$$- 100R^7 + (180R^5 - 440R^6 - 260R^7 + 320R^8 + 200R^9)\ln R + \delta R(1+R)^3(20 + 25R - 40R^2$$
$$+ 25R^3 + 20R^4 - 50R^5)\ln\tilde{\delta}). \quad \text{(B28)}$$

APPENDIX C: Δ(1232) ELECTROMAGNETIC FORM FACTORS

For the nucleon electromagnetic form factors we take the mass scale $M_{sc} = M_\Delta$.
The following functions occur in the Feynman-graphs of Fig. 2:

$$\tilde{\mathcal{M}}_1 = z\mu^2 + (1-z)^2, \qquad \tilde{\mathcal{M}}_2 = (1-z)\mu^2 + z^2, \qquad \tilde{\mathcal{M}}_3 = z\mu^2 + (1-z)r^2 - z(1-z),$$
$$\tilde{\mathcal{M}}_4 = (1-z)\mu^2 + zr^2 - z(1-z), \qquad \tilde{\mathcal{M}}_{56} = z\mu^2 + (1-z)^2. \quad \text{(C1)}$$

For better reading we introduce the functions:

$$\tilde{J}_1(\tilde{\mathcal{M}}) = \tilde{\mathcal{M}}[L - 1 + \ln\tilde{\mathcal{M}}], \qquad \tilde{J}_2(\tilde{\mathcal{M}}) = [L + \ln\tilde{\mathcal{M}}], \qquad \tilde{J}_3(\tilde{\mathcal{M}}) = \frac{1}{\tilde{\mathcal{M}}}. \tag{C2}$$

The isospin factors are given by:

$$I_1 = \begin{pmatrix} \frac{2}{3} \\ \frac{2}{9} \\ -\frac{2}{9} \\ -\frac{2}{3} \end{pmatrix} \quad I_2 = \begin{pmatrix} \frac{8}{3} \\ \frac{13}{9} \\ \frac{2}{9} \\ -1 \end{pmatrix} \quad I_3 = \begin{pmatrix} 1 \\ \frac{1}{3} \\ -\frac{1}{3} \\ -1 \end{pmatrix} \quad I_4 = \begin{pmatrix} 1 \\ \frac{2}{3} \\ \frac{1}{3} \\ 0 \end{pmatrix} \quad I^a_{56} = \begin{pmatrix} \frac{2}{3} \\ \frac{2}{9} \\ -\frac{2}{9} \\ -\frac{2}{3} \end{pmatrix} \quad I^b_{56} = \begin{pmatrix} \frac{8}{3} \\ \frac{13}{9} \\ \frac{2}{9} \\ -1 \end{pmatrix} \quad I_T = \begin{pmatrix} \frac{2}{3} \\ \frac{2}{9} \\ -\frac{2}{9} \\ -\frac{2}{3} \end{pmatrix} \tag{C3}$$

In order to project on the individual Lorentz-structures we use the following identities:

$$\begin{aligned} \bar{u}_\alpha(p')\gamma^\mu u^\alpha(p) &= \frac{1}{2M_\Delta}\bar{u}_\alpha(p')[n^\mu - \gamma^{\mu\nu}q_\nu]u^\alpha(p) \\ \bar{u}_\alpha(p')[q^\alpha g^{\mu\beta} - q^\beta g^{\mu\alpha}]u_\beta(p) &= \bar{u}_\alpha(p')\Big[2M_\Delta(1+\tau)g^{\alpha\beta}\gamma^\mu - g^{\alpha\beta}n^\mu + \frac{1}{M_\Delta}q^\alpha q^\beta\gamma^\mu\Big]u_\beta(p), \end{aligned} \tag{C4}$$

with $n = p' + p$. The first one is the Gordon-identity for Δ spinors and the second a Δ spinor identity given, e.g. in [64].

In the following subsections we give the individual contributions from the Feynman-diagrams of Fig. 2 to the $\Delta(1232)$-isobar form factors. We only list nonvanishing contributions. These are the nonrenormalized expressions.

1. Contributions to $F_2^\Delta(0)$

$$\begin{aligned} F_2^{\Delta 1}(0) &= C_{\Delta\Delta}I_1\int_0^1 dz 2z\Big[\frac{5}{6} - \frac{1}{3}z - \frac{7}{6}z^2 - \epsilon_d\Big(\frac{13}{9} - \frac{4}{9}z - \frac{17}{9}z^2\Big)\Big]\tilde{J}_2(\tilde{\mathcal{M}}_1) \\ F_2^{\Delta 2}(0) &= C_{\Delta\Delta}I_2\int_0^1 dz 2z\Big\{-\Big[-\frac{1}{9} + \frac{5}{9}z + \epsilon_d\Big(\frac{11}{27} - \frac{199}{108}z\Big)\Big]\tilde{J}_1(\tilde{\mathcal{M}}_2) - \Big[-\frac{4}{9} + 3z - \frac{5}{3}z^2 + \frac{5}{36}z^3 \\ &\quad + \epsilon_d\Big(\frac{32}{27} - \frac{50}{9}z + \frac{10}{3}z^2 - \frac{23}{54}z^3\Big)\Big]\tilde{J}_2(\tilde{\mathcal{M}}_2)\Big\} \\ F_2^{\Delta 3}(0) &= C_{N\Delta}I_3\int_0^1 dz 2z\Big\{-\Big[-\frac{1}{2}z + z^2 - \frac{1}{2}r + zr\Big]\tilde{J}_2(\tilde{\mathcal{M}}_3)\Big\} F_2^{\Delta 4}(0) = C_{N\Delta}I_4\int_0^1 dz 2z\{-[z - z^2 + rz]\tilde{J}_2(\tilde{\mathcal{M}}_4)\} \end{aligned} \tag{C5}$$

Nonminimal contribution to $\Delta 2$ with $\kappa_1 = \kappa_2 = \kappa_{nm}$ (without the $\gamma^{\beta\delta\gamma}$ part):

$$\begin{aligned} F_2^{\Delta 2}(0) = \kappa_{nm}C_{\Delta\Delta}I_2\int_0^1 dz 2z\Big\{&-\Big[\frac{47}{18} - \frac{8}{9}z + \epsilon_d\Big(-\frac{271}{54} + \frac{70}{27}z\Big)\Big]\tilde{J}_1(\tilde{\mathcal{M}}_2) \\ &-\Big[\frac{22}{9} - \frac{10}{3}z + \frac{3}{2}z^2 - \frac{2}{9}z^3 + \epsilon_d\Big(-\frac{188}{27} + \frac{28}{3}z - \frac{37}{9}z^2 + \frac{16}{27}z^3\Big)\Big]\tilde{J}_2(\tilde{\mathcal{M}}_2)\Big\} \end{aligned} \tag{C6}$$

2. Contributions to $F_3^\Delta(0)$

$$\begin{aligned} F_3^{\Delta 1}(0) &= C_{\Delta\Delta}I_1\int_0^1 dz 2z\Big\{[3 - 2\epsilon_d]\tilde{J}_1(\tilde{\mathcal{M}}_1) - \Big[4 + \frac{2}{3}z - \frac{70}{9}z^2 + \epsilon_d\Big(-\frac{44}{9}z + \frac{76}{27}z^2\Big)\Big]\tilde{J}_2(\tilde{\mathcal{M}}_1) - \frac{8}{9}z^2[1 - z^2]\tilde{J}_3(\tilde{\mathcal{M}}_1)\Big\} \\ F_3^{\Delta 2}(0) &= C_{\Delta\Delta}I_2\int_0^1 dz 2z\Big\{-\Big[-\frac{5}{3} + \frac{2}{9}z + \epsilon_d\Big(-\frac{10}{3} - \frac{59}{54}z\Big)\Big]\tilde{J}_1(\tilde{\mathcal{M}}_2) - \Big[\frac{16}{3} - \frac{104}{9}z + 5z^2 + \frac{1}{18}z^3 \\ &\quad + \epsilon_d\Big(\frac{32}{9} + \frac{88}{27}z - \frac{174}{27}z^2 - \frac{7}{27}z^3\Big)\Big]\tilde{J}_2(\tilde{\mathcal{M}}_2) - \Big[\frac{16}{9}z^2 - \frac{16}{9}z^3 + \frac{4}{9}z^4\Big]\tilde{J}_3(\tilde{\mathcal{M}}_1)\Big\} \\ F_3^{\Delta 3}(0) &= C_{N\Delta}I_3\int_0^1 dz 2z\Big\{-\Big[\frac{4}{3}z^2 + rz\Big]\tilde{J}_2(\tilde{\mathcal{M}}_3) + \Big[\frac{2}{3}z^3 - \frac{2}{3}z^4 + \frac{2}{3}rz^2 - \frac{2}{3}rz^3\Big]\tilde{J}_3(\tilde{\mathcal{M}}_3)\Big\} \\ F_3^{\Delta 4}(0) &= C_{N\Delta}I_4\int_0^1 dz 2z\Big\{-\Big[z + rz - \epsilon_d\frac{1}{3}z^2\Big]\tilde{J}_2(\tilde{\mathcal{M}}_3) - \Big[-\frac{1}{3}z^2 + \frac{2}{3}z^3 - \frac{1}{3}z^4 - \frac{2}{3}rz^2 - \frac{1}{3}r^2z^2 + \frac{2}{3}rz^3\Big]\tilde{J}_3(\tilde{\mathcal{M}}_4)\Big\} \\ F_3^{\Delta 56}(0) &= C_{\Delta\Delta}I^a_{56}\int_0^1 dx[4 + 6z - \epsilon_d 4z]\tilde{J}_1(\tilde{\mathcal{M}}_{56}) + C_{\Delta\Delta}I^b_{56}\int_0^1 dx\frac{1}{9}[12 + 48z + \epsilon_d(44 - 28z)]\tilde{J}_1(\tilde{\mathcal{M}}_{56}) \end{aligned} \tag{C7}$$

Nonminimal contribution to $\Delta 2$ with $\kappa_1 = \kappa_2 = \kappa_{nm}$ (without the $\gamma^{\beta\delta\gamma}$ part):

$$F_3^{\Delta 2}(0) = \kappa_{nm} C_{\Delta\Delta} I_2 \int_0^1 dz 2z \Big\{ \Big[\Big[4 - \frac{28}{9} z - \epsilon_d \Big(- \frac{118}{9} - \frac{269}{27} z \Big) \Big] \tilde{J}_1(\tilde{\mathcal{M}}_2) - \Big[\frac{8}{3} + \frac{8}{9} z - \frac{8}{3} z^2 + \frac{7}{9} z^3 + \epsilon_d \Big(- \frac{272}{9} + \frac{704}{27} z - \frac{8}{9} z^2 - \frac{62}{27} z^3 \Big) \Big] \tilde{J}_2(\tilde{\mathcal{M}}_2) \Big\} \tag{C8}$$

3. Contributions to $F_4^{\Delta}(0)$

$$F_4^{\Delta 1}(0) = C_{\Delta\Delta} I_1 \int_0^1 dz 2z \Big\{ [4 - 8z^2 - \epsilon_d 4z(1-z)] \tilde{J}_2(\tilde{\mathcal{M}}_1) + \frac{8}{9} z^2 [1 - z^2] \tilde{J}_3(\tilde{\mathcal{M}}_1) \Big\}$$

$$F_4^{\Delta 2}(0) = C_{\Delta\Delta} I_2 \int_0^1 dz 2z \Big\{ - \Big[\frac{128}{9} z - 8z^2 - \frac{10}{27} z^3 + \epsilon_d \Big(- \frac{64}{27} z + \frac{104}{27} z^2 + \frac{86}{81} z^3 \Big) \Big] \tilde{J}_2(\tilde{\mathcal{M}}_2) - \Big[- \frac{32}{27} z^2 + \frac{16}{9} z^3 - \frac{4}{9} z^4 - \frac{2}{27} z^5 \Big] \tilde{J}_3(\tilde{\mathcal{M}}_2) \Big\}$$

$$F_4^{\Delta 3}(0) = C_{N\Delta} I_3 \int_0^1 dz 2z \Big\{ - \frac{2}{3} [z^3 - z^4 + r z^2 - r z^3] \tilde{J}_3(\tilde{\mathcal{M}}_3) \}$$

$$F_4^{\Delta 4}(0) = C_{N\Delta} I_4 \int_0^1 dz 2z \Big\{ - \frac{2}{3} [-z^3 + z^4 - r z^3] \tilde{J}_3(\tilde{\mathcal{M}}_4) \Big\} \tag{C9}$$

Nonminimal contribution to $\Delta 2$ with $\kappa_1 = \kappa_2 = \kappa_{nm}$ (without the $\gamma^{\beta\delta\gamma}$ part):

$$\frac{1}{\kappa} F_4^{\Delta 2}(0) = C_{\Delta\Delta} I_2 \int_0^1 dz 2z \Big\{ - \Big[16 - 8z + \epsilon_d \Big(- \frac{16}{3} + \frac{38}{3} z \Big) \Big] \tilde{J}_1(\tilde{\mathcal{M}}_2) - \Big[- \frac{152}{9} z + \frac{112}{9} z^2 - \frac{74}{27} z^3 + \epsilon_d \Big(\frac{544}{27} z - \frac{136}{9} z^2 + \frac{148}{81} z^3 \Big) \Big] \tilde{J}_2(\tilde{\mathcal{M}}_2) - \Big[\frac{32}{27} z^2 - \frac{16}{9} z^3 + \frac{8}{9} z^4 - \frac{4}{27} z^5 \Big] \tilde{J}_3(\tilde{\mathcal{M}}_2) \Big\} \tag{C10}$$

4. Contributions to the charge radius $\langle r_{E0}^2 \rangle$

$$\frac{d}{dq^2}\Big|_{q^2=0} F_1^{\Delta 1} = - \frac{C_{\Delta\Delta}}{M_\Delta^2} I_1 \int_0^1 dz 2z \frac{1}{216} \Big\{ -132z + 110z^2 - 27\tilde{\mathcal{M}}_1 + [-66z^2 + 66z^4] \frac{1}{\tilde{\mathcal{M}}_1} + [-108 - 18z + 231z^2] \ln \tilde{\mathcal{M}}_1 + 81 \tilde{\mathcal{M}}_1 \ln \tilde{\mathcal{M}}_1 \Big\}$$

$$\frac{d}{dq^2}\Big|_{q^2=0} F_1^{\Delta 2} = - \frac{C_{\Delta\Delta}}{M_\Delta^2} I_2 \int_0^1 dz 2z \frac{1}{216} \Big\{ -[-128 + 192z - 113z^2 + 23z^3] - \Big[128 + \frac{139}{2} z \Big] \tilde{\mathcal{M}}_2 + [-132z^2 + 132z^3 - 33z^4] \frac{1}{\tilde{\mathcal{M}}_2} + \Big[-132 + 216z - 15z^2 - \frac{15}{2} z^3 \Big] \ln \tilde{\mathcal{M}}_2 + [51 - 30z] \tilde{\mathcal{M}}_2 \ln \tilde{\mathcal{M}}_2 \Big\}$$

$$\frac{d}{dq^2}\Big|_{q^2=0} F_1^{\Delta 3} = - \frac{C_{N\Delta}}{M_\Delta^2} I_3 \int_0^1 dz 2z \frac{1}{24} \Big\{ -z^2 2[z - z^2 + r - rz] \frac{1}{\tilde{\mathcal{M}}_3} + [-2z^2 - 3rz] \ln \tilde{\mathcal{M}}_3 \Big\}$$

$$\frac{d}{dq^2}\Big|_{q^2=0} F_1^{\Delta 4} = - \frac{C_{N\Delta}}{M_\Delta^2} I_4 \int_0^1 dz 2z \frac{1}{24} \Big\{ +z^2 - z^2[1 - 2z + z^2 + 2r - 2rz + r^2] \frac{1}{\tilde{\mathcal{M}}_4} + [-3z + 6z^2 - 3rz] \ln \tilde{\mathcal{M}}_4 \Big\}$$

$$\frac{d}{dq^2}\Big|_{q^2=0} F_1^{\Delta T12} = - \frac{2}{3} \frac{C_{\Delta\Delta}}{H_A^2 M_\Delta^2} I_T \ln(\mu^2) \tag{C11}$$

Nonminimal contribution to $\Delta 2$ with $\kappa_1 = \kappa_2 = \kappa_{nm}$ (without the $\gamma^{\beta\delta\gamma}$ part):

$$\frac{d}{dq^2}\Big|_{q^2=0} F_1^{\Delta 2} = - \kappa_{nm} \frac{C_{\Delta\Delta}}{M_\Delta^2} I_2 \int_0^1 dz \frac{2z}{108} \{ -472 + 676z - 236z^2 + 8z^3 - [225 - 23z] \tilde{\mathcal{M}}_2 + [-60 + 42z - 12z^2 + 3z^3] \ln \tilde{\mathcal{M}}_2 + [54 + 12z] \tilde{\mathcal{M}}_2 \ln \tilde{\mathcal{M}}_2 \} \tag{C12}$$

5. Renormalized constants

The constants are with $\bar{\delta} = \delta^2 (1 + r)^2$:

$$c_\mu = r\frac{C_{\Delta\Delta}}{972}(-965-1781\kappa_{nm}) - r\frac{C_{N\Delta}}{36\delta}(-12-28r-18\mu^2 r+28r^2+54r^3-15r^4-51r^5+6r^6 + 18r^7-12r^3(-8+4r+13r^2-3r^3-10r^4+r^5+3r^6)\ln r + (3+6r-9r^2-24r^3 + 12r^4+39r^5-9r^6-30r^7+3r^8+9r^9)\ln\bar{\delta}), \tag{C13}$$

$$c_{\mathcal{Q}} = \frac{C_{\Delta\Delta}}{243}(-604-4121\kappa_{nm}) + \frac{C_{N\Delta}}{18}\Big(4r^2(-4-2r+4r^2-2r^3-4r^4+3r^5+3r^6)\ln r + \frac{1}{\delta^2}(11-13r-13r^2 + 22r^3-3r^4-15r^5+11r^6+6r^7-6r^8-\bar{\delta}(3-3r-r^2+3r^3-r^4-3r^5+3r^6)\ln\bar{\delta})\Big), \tag{C14}$$

$$c_{\mathcal{O}} = \frac{C_{\Delta\Delta}}{2916}(-6247+20293\kappa_{nm}) - \frac{C_{N\Delta}}{36\delta(1+r)}(-8-10r+2r^3+7r^4+20r^5+7r^6-12r^7-6r^8 + 4r(-8+12r^2+4r^3+3r^4-2r^5-13r^6-5r^7+6r^8+3r^9)\ln r - \bar{\delta}(-3-5r-3r^2-r^3+r^4+6r^5+3r^6)\ln\bar{\delta}), \tag{C15}$$

$$c_{r0} = \frac{C_{\Delta\Delta}}{1944M_\Delta^2\bar{\delta}}(3850-7700r+3850r^2+(-5395+10790r-5395r^2)\kappa_{nm}) + \frac{C_{N\Delta}}{1944M_\Delta^2}\Big((-4320r^2-2160r^3+4320r^4-1188r^5-367\upsilon\upsilon 2r^6+3240r^7+3240r^8)\ln r + \frac{1}{\delta^2}(2268-3078r-2430r^2+4806r^3-324r^4-3888r^5+2646r^6+1620r^7-1620r^8 + (-648+729r+1566r^2-2187r^3-1080r^4+2997r^5-756r^6-2349r^7+1728r^8+810r^9-810r^{10})\ln\bar{\delta})\Big). \tag{C16}$$

APPENDIX D: NUCLEON AND Δ(1232) MASSES

In Sec. V we use the pion mass dependent nucleon and Δ(1232) masses of [46]:

$$M_N(m_\pi^2) = \mathring{M}_N - 4c_{1N}m_\pi^2 + \Sigma_N(m_\pi^2)$$
$$\Sigma_N(m_\pi^2) = -\frac{3g_A^2}{(8\pi f_\pi)^2}m_\pi^3\Big[4\Big(1-\frac{m_\pi^2}{4\mathring{M}_N^2}\Big)^{5/2}\arccos\frac{m_\pi}{2\mathring{M}_N} + \frac{17m_\pi}{16\mathring{M}_N} - \Big(\frac{m_\pi}{2\mathring{M}_N}\Big)^3 + \frac{m_\pi}{8\mathring{M}_N}\Big(30-10\Big(\frac{m_\pi}{\mathring{M}_N}\Big)^2+\Big(\frac{m_\pi}{\mathring{M}_N}\Big)^4\Big)\ln\Big(\frac{m_\pi}{\mathring{M}_N}\Big)\Big] \tag{D1}$$

$$M_\Delta(m_\pi^2) = \mathring{M}_\Delta - 4c_{1\Delta}m_\pi^2 + \mathrm{Re}\,\Sigma_\Delta(m_\pi^2), \tag{D2}$$

$$\Sigma_\Delta(m_\pi^2) = -\frac{1}{2}\Big(\frac{h_A}{8\pi\mathring{f}_\pi}\Big)^2\mathring{M}_\Delta^3(V_1-V_2-\mu^2V_3) \tag{D3}$$

$$V_1 = \int_0^1 dx(r+x)(\mu^2x+(1-x)(r^2-x))\mathrm{Log}[\mu^2x+(1-x)(r^2-x)]$$
$$V_2 = \frac{5}{36}+\frac{5}{18}r-\frac{7}{36}r^2-\frac{2}{3}r^3-\frac{1}{8}r^4+\frac{1}{6}r^5+\frac{1}{12}r^6-\frac{1}{6}r^5(r^3+2r^2-2r-6)\ln r+\frac{1}{12}(r^2-1)^3(1+r)^2\ln[1-r^2]$$
$$V_3 = \frac{1}{18}(7+9r+3r^2+9r^3+6r^4)+\frac{1}{3}r^5(3+2r)\ln r = +\frac{1}{3}\Big(1+\frac{3}{2}r-\frac{3}{2}r^5-r^6\Big)\ln[1-r^2] \tag{D4}$$

with $\mu = m_\pi/\mathring{M}_\Delta$, $r = \mathring{M}_N/\mathring{M}_\Delta$.

[1] R. Hofstadter and R. W. McAllister, Phys. Rev. **98**, 217 (1955).
[2] R. Hofstadter, Rev. Mod. Phys. **28**, 214 (1956).
[3] R. Pohl *et al.*, Nature (London) **466**, 213 (2010).
[4] J. C. Bernauer *et al.*, Phys. Rev. Lett. **105**, 242001 (2010).
[5] U. D. Jentschura, Ann. Phys. (N.Y.) **326**, 516 (2011).
[6] M. O. Distler, J. C. Bernauer, and T. Walcher, Phys. Lett. B **696**, 343 (2011).
[7] C. E. Carlson and M. Vanderhaeghen, Phys. Rev. A **84**, 020102 (2011).
[8] G. A. Miller, A. W. Thomas, J. D. Carroll, and J. Rafelski, Phys. Rev. A **84**, 020101 (2011).
[9] P. Mergell, U. G. Meissner, and D. Drechsel, Nucl. Phys. **A596**, 367 (1996).
[10] H. W. Hammer, Eur. Phys. J. A **28**, 49 (2006).
[11] S. Pacetti, Eur. Phys. J. A **32**, 421 (2007).
[12] H. W. Hammer and U. G. Meissner, Eur. Phys. J. A **20**, 469 (2004).
[13] M. A. Belushkin, H. W. Hammer, and U. G. Meissner, Phys. Lett. B **633**, 507 (2006).
[14] S. Weinberg, Physica A (Amsterdam) **96**, 327 (1979).
[15] J. Gasser and H. Leutwyler, Ann. Phys. (N.Y.) **158**, 142 (1984).
[16] T. Yamazaki, Y. Aoki, T. Blum, H.-W. Lin, S. Ohta *et al.* (RBC and UKQCD Collab.), Phys. Rev. D **79**, 114505 (2009).
[17] S. N. Syritsyn, J. D. Bratt, M. F. Lin, H. B. Meyer, J. W. Negele *et al.* (LHPC Collab.), Phys. Rev. D **81**, 034507 (2010).
[18] C. Alexandrou, M. Brinet, J. Carbonell, M. Constantinou, P. A. Harraud *et al.*, Phys. Rev. D **83**, 094502 (2011).
[19] S. Collins *et al.*, Phys. Rev. D **84**, 074507 (2011).
[20] J. D. Bratt *et al.* (LHPC Collab.), Phys. Rev. D **82**, 094502 (2010).
[21] C. Aubin, K. Orginos, V. Pascalutsa, and M. Vanerhaeghen, Phys. Rev. D **79**, 051502 (2009).
[22] C. Alexandrou *et al.*, Phys. Rev. D **79**, 014507 (2009).
[23] C. Alexandrou *et al.*, Nucl. Phys. **A825**, 115 (2009).
[24] C. Alexandrou *et al.*, Proc. Sci., CD09 (2011) 094502.
[25] C. Alexandrou, G. Koutsou, J. W. Negele, Y. Proestos, and A. Tsapalis, Phys. Rev. D **83**, 014501 (2011).
[26] E. E. Jenkins and A. V. Manohar, Phys. Lett. B **255**, 558 (1991).
[27] T. Becher and H. Leutwyler, Eur. Phys. J. C **9**, 643 (1999).
[28] V. Pascalutsa, in *Baryons 2010*, AIP Conf. Proc. No. 1388 (AIP, New York, 2011).
[29] J. Gegelia, G. Japardize, and X. Q. Wang, J. Phys. G **29**, 2303 (2003).
[30] T. Fuchs, J. Gegelia, G. Japardize, and S. Scherer, Phys. Rev. D **68**, 056005 (2003).
[31] T. Ledwig, V. Pascalutsa, and M. Vanderhaeghen, Phys. Lett. B **690**, 129 (2010).
[32] V. Bernard, H. W. Fearing, T. R. Hemmert, and U. G. Meissner, Nucl. Phys. **A635**, 121 (1998).
[33] F. J. Jiang and B. C. Tiburzi, Phys. Rev. D **81**, 034017 (2010).
[34] B. Kubis and U. G. Meissner, Nucl. Phys. A **679**, 698 (2001).
[35] N. Kaiser, Phys. Rev. C **68**, 025202 (2003).
[36] T. Fuchs, J. Gegelia, and S. Scherer, J. Phys. G **30**, 1407 (2004).
[37] L. S. Geng, J. Martin-Camalich, and M. J. Vicente Vacas, Phys. Rev. Lett. **101**, 222002 (2008).
[38] L. S. Geng, J. Martin-Camalich, M. J. Vicente Vacas, Phys. Lett. B **676**, 63 (2009).
[39] L. S. Geng, J. Martin-Camalich, M. J. Vicente Vacas, Phys. Rev. D **80**, 034027 (2009).
[40] J. Gasser, M. E. Sainio, and A. Svarc, Nucl. Phys. **B307**, 779 (1988).
[41] M. R. Schindler, J. Gegelia, and S. Scherer, Phys. Lett. B **586**, 258 (2004).
[42] T. R. Hemmert, B. R. Holstein, and J. Kambor, Phys. Lett. B **395**, 89 (1997).
[43] V. Pascalutsa and D. R Phillips, Phys. Rev. C **67**, 055202 (2003).
[44] B. Long and U. van Kolck, Nucl. Phys. **A840**, 39 (2010).
[45] V. Pascalutsa, M. Vanderhaeghen, and S. N. Yang, Phys. Rep. **437**, 125 (2007).
[46] V. Pascalutsa and M. Vanderhaeghen, Phys. Lett. B **636**, 31 (2006).
[47] V. Pascalutsa, Phys. Rev. D **58**, 096002 (1998).
[48] V. Pascalutsa and R. Timmermans, Phys. Rev. C **60**, 042201 (1999).
[49] V. Pascalutsa, Phys. Lett. B **503**, 85 (2001).
[50] S. Deser, V. Pascalutsa, and A. Waldron, Phys. Rev. D **62**, 105031 (2000).
[51] C. Lorce, Phys. Rev. D **79**, 113011 (2009).
[52] V. Bernard *et al.*, Nucl. Phys. **A635**, 121 (1998).
[53] C. Amsler *et al.* (Particle Data Group), Phys. Lett. B **667**, 1 (2008).
[54] M. A. Belushkin, H.-W. Hammer, and U.-G. Meissner, Phys. Rev. C **75**, 035202 (2007).
[55] V. Bernard, H. W. Fearing, T. R. Hemmert, and U. G. Meissner, Nucl. Phys. **A635**, 121 (1998).
[56] A. I. Machavariani, A. Fäßler, and A. J. Buchmann, Nucl. Phys. **A646**, 231 (1999); **A686**, 601 (2001).D. Drechsel *et al.*, Phys. Lett. B **484**, 236 (2000).D. Drechsel and M. Vanderhaeghen, Phys. Rev. C **64**, 065202 (2001).
[57] A. J. Buchmann, J. A. Hester, and R. F. Lebed, Phys. Rev. D **66**, 056002 (2002).
[58] L. Tiator, D. Drechsel, S. S. Kamalov, and S. N. Yang, Eur. Phys. J. A **17**, 357 (2003).
[59] T. Ledwig, V. Pascalutsa, and M. Vanderhaeghen, Phys. Rev. D **82**, 091301 (2010).
[60] F. X. Lee, R. Kelly, L. Zhou, and W. Wilcox, Phys. Lett. B **627**, 71 (2005).
[61] G. Ramalho, M. T. Pena, and F. Gross, Phys. Rev. D **81**, 113011 (2010).
[62] S. R. Beane, Nucl. Phys. **B695**, 192 (2004).
[63] T. R. Hemmert, M. Procura, and W. Weise, Phys. Rev. D **68**, 075009 (2003).
[64] S. Nozawa and D. B. Leinweber, Phys. Rev. D **42**, 3567 (1990).